EXPLORING VARIATION OF FEMALE GENITAL MORPHOLOGY IN *HYDROLAGUS COLLIEI* (SPOTTED RATFISH)

by

Jennifer Garcia-Israel

A paper presented to the

Faculty of Mount Holyoke College in

Partial Fulfillment of the Requirements for

the Degree of Bachelors of Arts with

Honor

Department of Biological Sciences

South Hadley, MA 01075

May 2024

This paper was prepared

under the direction of

Professor Patricia Brennan

for eight credits.

ACKNOWLEDGEMENTS

I would like to first and foremost thank Dr. Patricia Rodriguez Brennan for her help, support and mentorship throughout this process. Since joining the Brennan lab two years ago, I have gained invaluable experiences and amazing insight into scientific research. I am incredibly grateful for her guidance and advice.

Thank you to Dr. Brandon Hedrick from Cornell University for developing the code used for statistical analysis in R Studio. A big thank you to Dr. Rachel Keeffe for her mentorship and help with 3D reconstruction and Adobe Illustrator.

Thank you to members of the Brennan lab for their assistance with scanning and raw data collection. I would also like to thank the past members of the Brennan lab, especially Kaitlyn Puorro, Valeria Serna-Solis, and Genesis Lara Granados for laying the groundwork for this study, be it through past codes or past research on ratfish. Thank you to Dr. Heather Hamilton for her advice on microscopy. I would also like to thank Dr. Jason Andras for allowing me to use his dissecting microscope. Thank you to my thesis committee members, Dr. Gary Gillis and Dr. Catherine Le Gouis, for reviewing my thesis and for their questions and feedback.

Finally, thank you to my family and friends for their love and support.

Baruch Hashem.

TABLE OF CONTENTS

List of Figures

Page

List of Tables

Page

ABSTRACT

Female genitalia are found to be more diverse than previously thought, yet they have been historically understudied in the scientific world. *Hydrolagus colliei* is a particularly interesting model for studying female genital morphology. Female ratfish have paired vaginal openings, as well as a paired vagina and oviducts. We investigated how female ratfish genital morphology varies through body size and ontogeny, and how the female ratfish genitalia may have coevolved with male ratfish genitalia by examining the histology of the vagina in females of different sizes. We also examined the anatomy of the anal pad, a fleshy structure present only in females on the ventral side of the tail. I found that the relationship between vaginal shape and body size is significant, vaginal thickness increases with size of the female ratfish, and that vaginal density does not appear to vary significantly. I also found that the anal pad has a thick layer of collagen that increases in thickness with body size. This study shows that vagina shape changes with body size in females, and that male and female genitalia are coevolving in ratfish. It also provides evidence that females evolve other specializations that differ from males, likely in a reproductive context.

INTRODUCTION

During copulation, the direct interaction of male and female genitalia in species with internal fertilization is possibly the most direct of evolutionary interactions between sexes. Due to the directness of this copulation, coevolution of male and female genital morphologies is expected (Brennan & Prum, 2015). This relationship between copulation and coevolution of genitalia is one of the reasons why studying genitalia is so interesting, as morphological changes in the genitalia of one sex can influence changes in the genitalia of the opposite sex, or mechanical constraints can prevent these changes (Brennan, 2016). As well as the connection between genitalia and evolution, the sheer diversity of genitalia is another compelling aspect of the study of genitalia.

Diversity in male and female genitalia is likely the result of natural and sexual selection. In addition, copulatory behavior is influenced by both natural selection and sexual selection. Since copulatory behavior and genital morphology are linked, it can be said that both natural selection and sexual selection influence genital morphology (Brennan & Orbach, 2020). However, sexual selection, more specifically post-copulatory sexual selection, is what generally influences or drives evolution of genital morphology (Brennan, 2016). Mechanisms of coevolution of genitalia include natural selection for mechanically feasible copulation, the lock-and-key hypothesis, female choice, male-male competition, and sexual conflict. Natural selection for mechanically feasible copulation means that the size and fit of genitalia in order to best copulate are selected for. The

lock-and-key hypothesis is to prevent hybridization, meaning that the male genitalia must fit into the female, as a “key” would fit into a “lock”. This is to ensure that a male of a different species will not mate with the female, preventing hybridization. Regarding the lock-and-key hypothesis, while it has not been falsified, there are other mechanisms that also result in genital coevolution, thus genital coevolution is not exclusive to the lock-and-key hypothesis. Another mechanism that can generate genital diversity is sexual selection through female choice. This refers to the female choosing their mate, thus mating preferences can affect the evolution of male genitalia, in order to be desirable for a female to mate with. Male-male competition is another additional mechanism of genital coevolution. It consists of males of the species competing to have a chance to copulate with a female. The males’ genitalia can thus evolve to increase their chance of copulation.

An important mechanism to note is sexual conflict, which results in sexually antagonistic coevolution. Because the evolutionary interests of males and females are not identical, each sex will try to maximize its own fitness at the expense of the other sex. For this reason, during mating, males may try to manipulate female reproduction to make sure they sire her offspring, while the female tries to reassert her own reproductive choice, sometimes mitigating the harm done by males. In this case, there are a variety of coevolved female morphological responses in genitalia to reduce damage done by male genitalia (Brennan & Prum, 2015).

One of the problems of studying genital coevolution is that female genitalia are often understudied (Orbach et al., 2018). While male genitalia have been recognized as having a lot of variation, it has been studied often without attention to their female counterparts (Ah-King et al., 2014). It is essential to study female genitalia, as increasingly more variation in female genitalia has been found, and studying female genitalia can help us to understand complex coevolution between sexes and how this affects variation in genitalia.

In this thesis, I will examine the female genitalia of *Hydrolagus colliei*, (spotted ratfish). This species belongs to the class Chondrichthyes, order Chimaeriformes, and family Chimaeridae (Johnson, 1967). The biology of chimaeroids, including the spotted ratfish, is less known and understood compared to all other major marine vertebrate groups (Cailliet & Ebert, 2014). Chondrichthyans are cartilaginous fish and their known habitats can range from freshwater riverine to the open sea (Cailliet & Ebert, 2014). Chimaeras' distribution is global and they can be found in both Pacific and Atlantic oceans (Didier & Rosenberger, 2002). The spotted ratfish in particular inhabits the Pacific Ocean off the west coast of the United States in shallow coastal waters, ranging from the surface to 971 m. *H. colliei* dwell at the bottom of these waters, usually in sandy or muddy bottoms (Didier et al., 2012). Spotted ratfish are also the most common species of chimaeras found off the west coast of the United States (Didier & Rosenberger, 2002).

Figure 1. Whole adult female ratfish specimen.

Characterized by their "conical fleshy snout", the ratfish, as well as chimaeras, have a unique appearance (Didier et al., 2012). Aside from the characteristic snout, spotted ratfish have cartilaginous skeletons and "elongate bodies, with long whip-like tails and smooth, scaleless skin" (Didier & Rosenberger, 2002). The ratfish have two dorsal fins, including their venomous spine, paired pectoral and pelvic fins, and a caudal fin (Didier et al., 2012), as seen in Figure 1 above.

In regards to food habits, the spotted ratfish has been described as "opportunist and feeds on what is available" (Johnson, 1967). While ratfish appear to mainly eat crustaceans, intercohort cannibalism has been observed as well (Johnson, 1967). Their teeth consist of three pairs of growing tooth plates that fuse together, and have the appearance of rodent incisors.

Ratfish are oviparous and deposit their eggs at the bottom of the ocean (Didier & Rosenberger, 2002). Gestation is estimated to be approximately 9-12 months in spotted ratfish (Dean, 1906). Studying their reproductive biology is

difficult but we know that ratfish extrude one or two egg cases during parturition (Barnett et al., 2009). Ratfish embryos are large and are encased in brown, heavy, “dart-shaped capsules” (Dean, 1906). The egg capsules are attached to the females for 24 hours before being deposited (Berio et al., 2023). Egg capsules are deposited in pairs every 2 weeks on average (Berio et al., 2023). There is not a clear seasonality to the ratfish reproductive cycle, however it has been found that egg case deposition occurs all year, with a maximum number of eggs deposited throughout July to September (Dean, 1906). It has also been observed in aquaria that the females spawn yearly but less frequently or not at all in October through January (Berio et al., 2023).

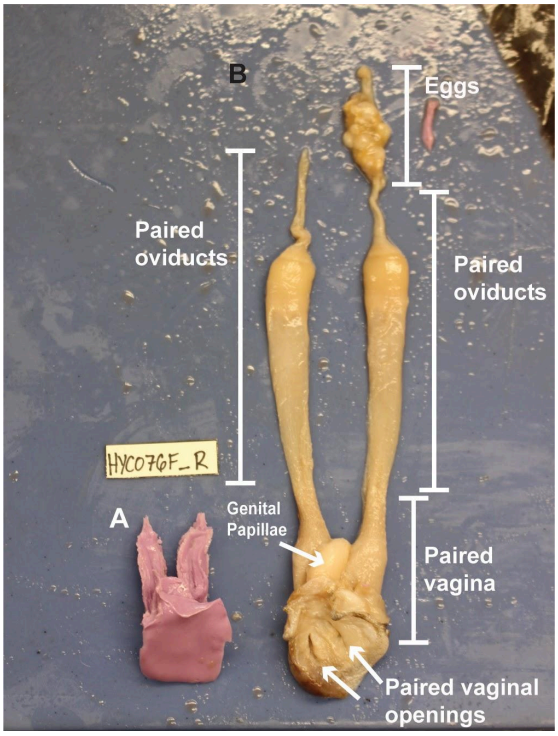

Figure 2. A. Adult vagina silicone model (left) B. Corresponding collected female reproductive tract (right), with labeled anatomy.

The variation of female genitalia as well as the genital morphology of *Hydrolagus colliei* (spotted ratfish) in particular have not been studied in depth. Literature existing on the genital morphology of *Hydrolagus colliei* and more broadly chondrichthyans, is discussed below, to work as a starting point for my research on the female genital morphology of the ratfish. Female ratfish have an internal reproductive tract, with paired oviducts, paired vaginal canals, genital papillae, and eggs when reproductive (Fig 2b). However, female spotted ratfish do not have a single cloacal opening like chondrichthyan fish, and amniotes except mammals, but rather have paired vaginal openings and a separate opening for the intestine (Fig 2b). This unique characteristic is not well understood. In 1963, Stanley published a study detailing the urogenital morphology of *Hydrolagus colliei*. They were the first to describe that female spotted ratfish had "paired vaginal openings" (Stanley, 1963) (Fig 2b).

According to Johnson (1967), the oviducal openings signify the age of the ratfish. Johnson also organizes the female ratfish in 3 groups: young, immature, and adult. Each group was classified by the absence or presence of the "oviducal openings"; young females did not have visible openings, immature females had small openings, and the adult females' oviducal openings were "open, elongated, and swollen" (Johnson, 1967).

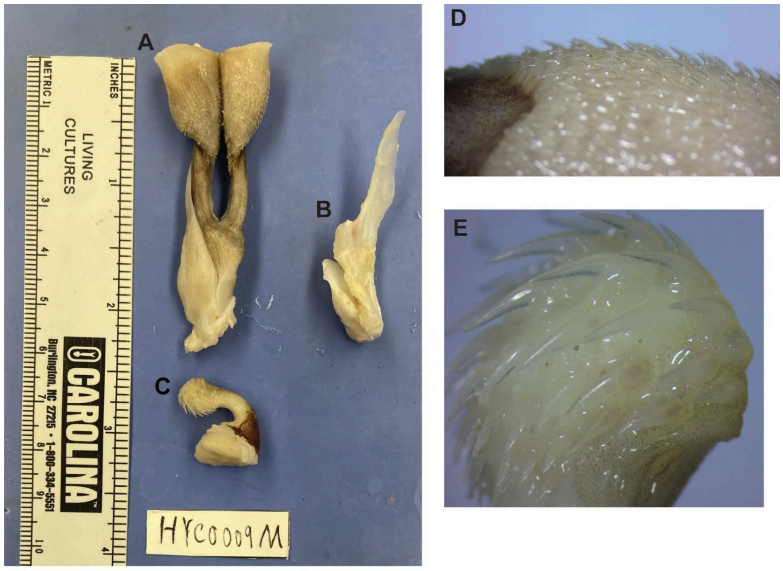

Figure 3. Male ratfish copulatory structures. (A) Paired claspers. (B) Pre-pelvic tenacula. (C) Frontal tenaculum (D) Paired clasper spines, photographed at 2x. (E) Frontal tenaculum spines, photographed at 2x.

Male ratfish have complex copulatory structures. Last year, Valeria Serna-Solis, my peer who worked in the Brennan lab, conducted research on integration and modularity of copulatory structures in male ratfish (*Hydrolagus colliei*) (Serna-Solis, 2022). Copulatory structures of the male ratfish include paired claspers, pre-pelvic tenacula, and a frontal tenaculum (Figure 3). The paired claspers are on the pelvic fins, they form from the most medial pelvic fin ray, and are located on the ventral part of the fish (Fig 3a). The claspers are shaped like a two-part prong, and there are two inflatable, spiny lobes at their tip (Fig 3d). Paired claspers function as the main intromittent organ, as during copulation the claspers are inserted inside the female's vaginal openings, and inflate. The paired pre-pelvic tenacula are located on the ventral side of the fish

and are anterior to the respective pelvic fins (Fig 3b). Their shape is like that of a blade and they extend from the pelvic girdle. Finally, the frontal tenaculum is located on the dorsal side of the head of the fish, and is essentially a curved structure with denticles at its tip (Didier, 1995)) (Fig 3c). The paired pre pelvic tenacula and the frontal tenaculum are used to latch on to the female during copulation (Didier, 1995). Figure 4 below provides a visual guide to ratfish copulation, based on the only instance of a description of this behavior from aquarium fish, and the copulatory structures are depicted in action.

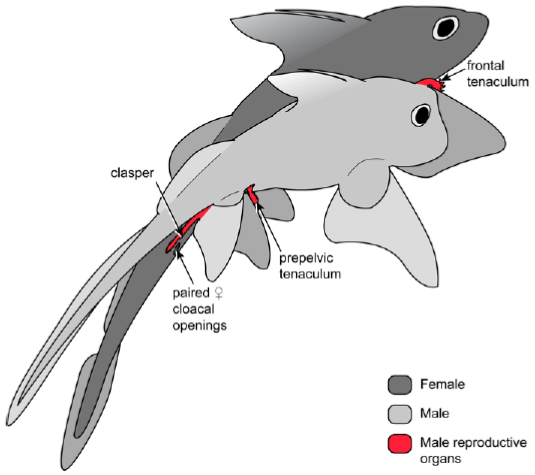

Figure 4. Ratfish copulation illustrated by Dr. Keeffe.

Serna-Solis (2022) found that in adults, there was no significant relationship between body size and the shape of the paired pelvic tenacula and claspers, but the relationship between body size and frontal tenaculum size was found to be significant. She also reported that copulatory structure's centroid size and shape changed suddenly rather than gradually in the transition from juvenile to adult ratfish. This pattern of growth is interesting because it has not been

detailed in vertebrate genitalia previously, and it suggests a rapid response to hormone changes in these structures (Serna-Solis, 2022).

While the genitalia and copulatory structures in male ratfish have been thus previously studied, there are no studies that focus on female ratfish genitalia. I seek to bridge this gap in the literature by researching the female genital morphology in *H. colliei*. I want to explore how the size and shape of female ratfish genitalia change as they age (juvenile vs adult) and determine if it is similar or different to that found in male ratfish. I predict that the females will change in their genital shape as they grow from juvenile to adult, as well as an increase in vaginal thickness and density of their tissues as they become adults, to mitigate the potential damage caused by the male clasper spines during copulation.

Because male ratfish use their spiny grasping frontal tenacula to hold on to the pectoral fin of female ratfish during copulation, I will investigate if female ratfish have evolved thicker skin on their pectoral fins compared to males using histology. I expect to find that the female fins will be thicker than the male fins. In sharks, where males bite the females during copulation, females have evolved thicker epidermis than in males (Crooks et al., 2013). Finally, the inflatable lobes of the claspers are full of small sharp spines in males, and these spines may abrade the female vaginal mucosa. Therefore, I expect that the tissue of the female vaginal canals in adults will be thicker than those of the juveniles, so that they can withstand the spines in the male's paired claspers.

My last research interest/question is to look into the function of the anal pad, which is a pad located on the ventral part of the tail in female ratfish. In the literature I have reviewed, no articles have mentioned the anal pad in *Hydrolagus colliei*, but has been mentioned in other closely related species. Mentions of an anal pad appear in the description of *Hydrolagus trolli, Chimaera orientalis, and Chimaera lignaria.* For *Hydrolagus trolli*, it is simply described as "an anal pad is present in females" (Didier, 2002). In the case of *Chimaera orientalis*, the anal pad is a "fleshy pad posterior to the cloaca, and is lacking in males" (Angulo et al., 2014). *Chimaera lignaria* also has these distinct anal pads in females (Didier, 2002). Thus, the anal pad is present in many female species close to *Hydrolagus colliei*, but no function has been suggested. I hypothesize that the anal pad is used as a cushion for the females to stabilize themselves during a female-specific activity, such as egg extrusion. Other possible functions could include being used while depositing eggs, or for other ecological purposes.

Statement of Purpose:

The aim of this paper is to examine and explore how female genital morphology in spotted ratfish varies. I aim to research what factors influence the shape of female ratfish genitalia, and how they may have coevolved with the several male counterpart copulatory structures and what evolutionary mechanisms could have driven this. My main research questions are: 1) How does the female genital morphology vary with body size and reproductive state , 2) How have

female ratfish genitalia coevolved with male ratfish genitalia?, and 3) What might the function of the female anal pad be?

MATERIALS AND METHODS

Specimens and Dissection

During this project we have dissected 36 female ratfish: 19 adults and 17 juveniles. I dissected thirty two female ratfish (15 adults and 17 juveniles) during the 2023 fall semester, with help from Dr. Brennan and students in the Brennan lab. The rest of the ratfish were dissected by other Brennan lab students in previous years. Three adult male ratfish were dissected in January of 2024. The ratfish specimens were obtained from a NOAA trawl survey in the Pacific Northwest in 2019.

Specimens were originally frozen, but when starting the process of dissection the specimens were thawed using cold water. Once thawed, various measurements were taken of the specimen and collected in a data sheet. Outer measurements included SVL (snout-vent length; vent being the vaginal openings), length 2 (length from vaginal openings to the end of the tail), dorsal spine length, anterior and posterior dorsal fin lengths (combined), the distal widths and lengths corresponding to the left and right pectoral and pelvic fins, and the length of the right and left vaginal openings' hole. Halfway through my dissections I noticed the anal pad and began to measure this structure in some of the females.

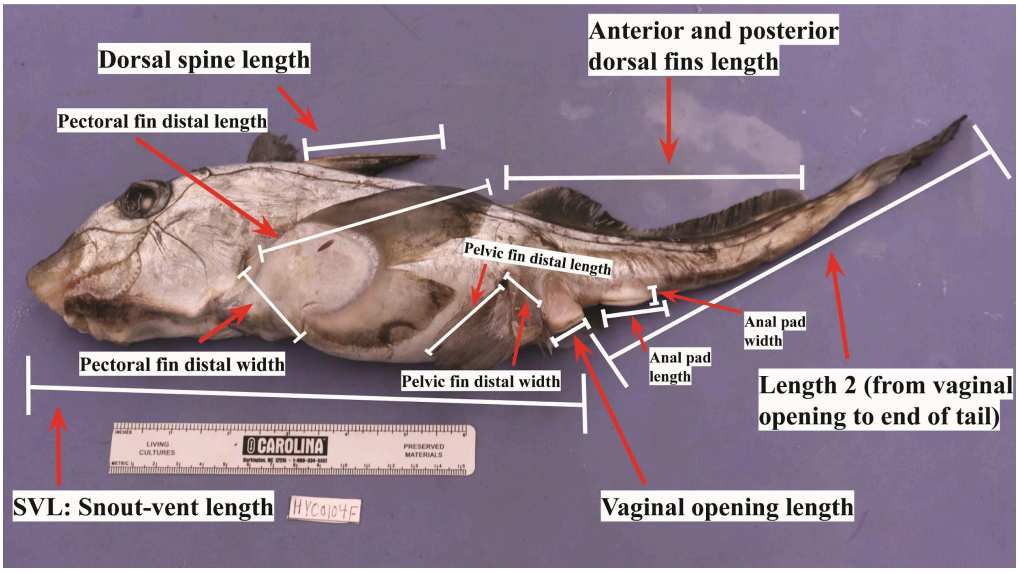

Figure 5. Adult female ratfish with outer measurements labeled

As seen in Figure 5, photos of the specimen with its label and a ruler for scale were also taken. After taking the outer measurements, the dissection proceeded by cutting the ventral part of the ratfish in a medial position. Then, various inner parts of the fish such as the liver, spleen, and stomach were removed in order to have a clear view of the reproductive tract. Measurements were then taken on the internal aspect; these measurements were paired vaginal lengths, oviduct lengths, diameter of the largest egg if present, and genital papillae length. We also recorded whether or not the ratfish was reproductive, which is determined by if the egg diameter is larger than 1 millimeter. All female macro anatomical measurements used were recorded in Table 4, Appendix A, and the measurements from the males were recorded in Table 5, Appendix A.

Next, silicone molds of the vagina were made as detailed below. We then collected both left and right pectoral and pelvic fins, the reproductive tract (from

the vaginal openings to the eggs), and the anal pad. The fins were wrapped in damp paper towels and stored in ziploc bags with corresponding labels. The reproductive tract and the ventral pad were stored in vials or jars, depending on size, and the container was filled with 10% formalin for preservation. Once tissues were collected, the specimen was disposed of into a biohazard bag.

Silicone Mold Technique

Silicone molds of the vagina were made using Zhermack Dental elite HD+ vinylpolysiloxane (a-silicone) impressions material. This silicone is traditionally used by dental offices for making molds. A silicone gun was used to push silicone into the paired vaginal openings, one at a time, until the vaginal canal was filled. A little silicone was also left on top of the paired holes, to create a base for the mold. Then the mold cured usually in 5 minutes, depending on the mucus and other secretions present in the tract of the fish. Once dry and deemed accurate in shape, the vaginal molds were stored in a plastic bag along with the corresponding specimen label. Shown below in Figure 6 is the technique used to create the mold.

Figure 6. Silicone technique

3D Modeling

To measure and quantify the shape of the vaginal structures, I made 3D models of the silicone molds using the Einscan Pro Handheld Scanner and *scAnt*, an open source platform for the creation of 3D models. For scanning large vaginal molds, the scanner was fixed in place and scanned the models as it turned on a turntable. After the scanning process was complete and editing such as plane cuts, applying mesh and watertight properties were done, the 3D model was saved as an OBJ file.

The next 3D modeling method, *scAnt*, was used for smaller specimens, so some juvenile vaginal molds were scanned using *scAnt*. *scAnt* is an open source platform for the creation of 3D models, and the machine in the Brennan lab was built by Sophia Smith, a student at Mount Holyoke during the summer of 2021, based on published instructions (Plum & Labonte, 2021). In order to use *scAnt*,

first the mold was placed in the inside of the lighted dome, and it was centered by controlling the x and z axes. The y axis is used for rotation of the specimen. Once specific parameters are set for the axes in order to center the specimen (mold), multiple photos are taken by the *scAnt* machine's camera. The parameters for *scAnt* when scanning juvenile vaginal models were inputted as the following via the graphic user interface (GUI):

Juvenile Vagina Model *scAnt* parameters	
Exposure: 70,000	**Threshold:** 3
Gain level: 3.83	Pitch (X axis): 150(min) - 250 (max)
Gamma: 0.8	Rotation (Y axis): 0-1600
Balance Ratio (red): 1.19	Focus (Z axis): -9,000 (max) - -14,000 (min)
Balance Ratio (blue): 3.1	Highlight Exposure: yes

Table 1. *scAnt* parameters

Raw photos were then stacked through commands using Python programming language. Stacked photos must then be masked, but before the masking step we edited the stacked photos in Adobe in order to crop the dark edges on the photos, so that the specimen can be clearly distinguished when masking. This method for using Adobe to ensure quality masking was developed

by Valeria Serna-Solis, a former student in the Brennan lab. Once the stacked photos are cropped using Adobe, masking of the photos is then conducted with Python once more. Then, using both the stacked and masked photos, a reconstruction was run through Zephyr 3D Lite, which is a photogrammetry software that uses the images input to create a 3D model output (Serna-Solis, 2022). If the reconstruction was successful, there would then be a digital 3D model of the juvenile ratfish vagina mold. The digital 3D model was then edited uniformly in order to be ready for analysis. *scAnt* was used only for scanning the largest 2 juvenile models.

The rest of the juvenile specimens were too small even for *scAnt*, so the main method used for scanning 12 models was CT scanning. 12 juvenile models were CT scanned using the Bruker SKYSCAN 1276 at the University of Massachusetts Amherst. The threshold parameter of the scan was 120-154. There were raw X-rays and then those files were reconstructed at Umass by Dr. Rachel Keeffe. Segmentation was then done at Mount Holyoke College using 3D Slicer, in order to obtain a final OBJ file of the juvenile specimens.

Editing Process for 3D models

Once the .obj file of the 3D model was created, the models were edited so they would be standardized. The base of the model was made minimal through a plane cut and oviducts were removed from the digital model. All edits to 3D models were made mainly with the use of Meshmixer software, as well as 3D

Slicer when needed. Because the models would not align during our Auto3dgm analysis, we added an asymmetric cross to the end of each specimen using Blender, so that the cross would help the software to align the models.

Geometric morphometrics method

To conduct the quantitative analysis of vaginal shape, we used Auto 3DGM. The method of Auto 3DGM stands for three-dimensional geometric morphometric landmarking. This automated software will automatically place points to comprise the specimen's shape, in order to align the different shapes of each specimen, compared to landmark-like feature points, which are difficult to identify across specimens, and subject to error (Boyer et al., 2015). The alignment of each specimen aided in comparing the shape, due to when the vaginal shapes were aligned, size was not a factor, as the specimens were to scale with each other. In order to align the specimens, the OBJ files of the vagina models were used as an input file to run Auto 3DGM in python from our lab computer. We used 200 low density landmarks and 3000 high density landmarks for the analysis. After the software analysis was complete, a visualization of alignment showed all the 3D models and their orientation. Because the original analysis did not properly align the specimens, we added an asymmetric alignment shape that helped the alignment process. We removed specimens 82J, 88J and 93F from the analysis because they would not align despite multiple attempts. Once in the

correct identical orientation, then the files can then be used for statistical analysis, as shown below in Figure 7.

Figure 7. Alignment of all vaginas via Auto3dgm

Statistical analysis of vagina models

Statistical analysis was conducted on the morphologika files that resulted from the Auto3dgm analysis. The morphologika files were text files that contain the geometric morphometric information of the vaginal shapes, such as the landmark data. RStudio (v2023.06.0) was used to create a plot and also conduct an ANOVA to analyze the variation of all the 3D models together. The code used was developed by Dr. Brandon Hedrick from Cornell University. The full code is found in Appendix D. The libraries loaded and used in R were geomorph, Morpho, and nlme. The morphologika.txt file for the juvenile and adult vaginas together was then read into R, and utilized as an input for running a generalized

procrustes analysis (GPA). To summarize the results of this analysis, the principal component analysis values (PCA) were used to obtain eigenvalues and variance. The values of PC1 and PC2 were plotted, as their proportion of variance was above 10%. The point colors on the produced plot ranged from red (large SVL) to blue (small SVL), as well as some points were purple, indicating an intermediate SVL value.

Point clouds of the vaginas were created using the PC1 and PC2 values. The purple point cloud depicted the negative axes for both PC1 and PC2; whereas, the green point cloud depicted the positive axes. An ANOVA was then conducted to determine whether there is a relationship between vaginal shape and corresponding size and ontogeny (juvenile or adult), as well as to analyze the significance of size and ontogeny on the vaginal shape.

Histology

Vaginal and anal pad tissues were prepared for paraffin histology and stained. The stains used for histology were Masson's Trichrome to visualize muscle and connective tissue, H&E to visualize nuclei and identify cells and elastin to determine if elastin fibers were present in the vaginal tissue.

I conducted paraffin histology on samples from 7 different specimens, 4 females and 3 males. The 3 males were all of similar size (HYCO110M, 111M, 112M) and the females varied in size, HYCO107F was a large adult female, HYCO102F was a juvenile, and HYCO085F and HYCO100F were medium-sized

adults. Samples included sections of the anal pad in both males and females, as well as the female vagina tract. Figures 8 and 9 show the location of where the vaginal and anal pad samples were taken from and how they were sectioned. Most reproductive tract samples were sagittal and transverse sectioned. Specifically, HYCO102F was not sectioned as it was an extremely small reproductive tract from a juvenile ratfish, and instead was placed whole in a cassette. All anal pad samples were transverse sectioned. Once sectioned, the samples were put in cassettes and stored in 10% formalin.

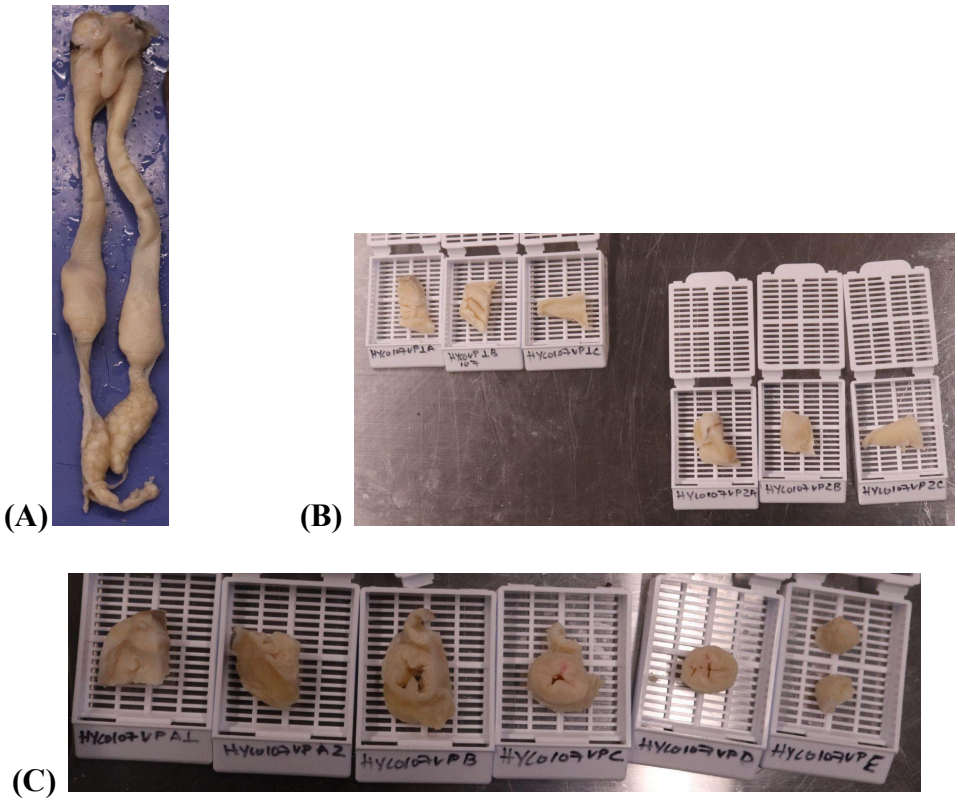

Figure 8. Example of reproductive tract sample preparation. (a) Whole reproductive tract (HYCO107F); (b) Sagittal sections of reproductive tract (HYCO107F); (c) Transverse sections of reproductive tract (HYCO107F)

(A) 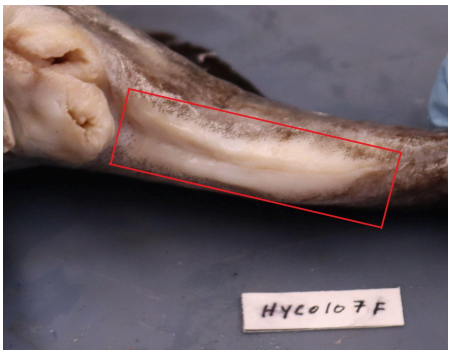

(B) 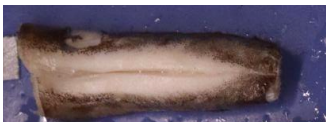

(C) 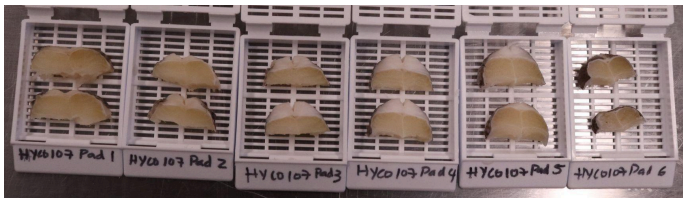

Figure 9. Example of anal pad sample preparation. (a) Location of anal pad in HYCO107F; (b) Anal pad sample (HYCO107F); (c) Transverse sections of anal pad sample in cassettes (HYCO107F)

In order to prepare the samples now in cassettes for histology, the standard paraffin histology protocol outlined in Table 7 (Appendix B) was followed. This protocol consists of dehydration, clearing, and infiltration prior to embedding and slicing. The embedded paraffin blocks of each sample were sliced using a Leico slicer at 7 μm. After getting adequate slices, each slice or ribbon of slices was mounted onto a slide and subsequently incubated overnight at 49.3 degrees Celsius. Approximately 3 slides were made for each sample. Some samples were not used as slices because they were not suitable, due to the tissue being dry and

hard to work with. For the anal pads, HYCO111M did not have samples used as the tissue was very dry.

Slides were then stained using Masson's Trichrome, Hematoxylin & Eosin, or Elastin stain. The protocols for each stain are outlined in Tables 8-10, Appendix B. Once stained with their respective stain, slides were preserved by applying 1-2 drops of Kleermount in Xylene to the slide and placing a glass coverslip on top. Slides were then ready for microscope use and imaging.

Imaging

Photographs of anal pad and vaginal pouch slides were taken using the Olympus BX51 microscope with a 5x objective. Pictures were adjusted for brightness and contrast within the program cellSens Standard. A constant scale bar of 500 μm was added when taking photos with a 5x objective. All slides photographed were stained with Masson's Trichrome, with the exception of tissue slices that were more complete in the H&E slide.

Measuring tissue microanatomy

Image J was used to analyze the thickness of the layers of vaginal and anal pad tissue. For the vaginal tissue, the thickness of the mucosal, collagenous, and muscularis layers were measured in Image J (Figure 10). Feret's diameter measurements were also used, and 8 measurements were taken per vaginal sample. In order to standardize these 8 measurements, 4 measurements were taken

at the symmetrical maximum points of the vagina and the other 4 measurements were taken at the minimum points. The average of the 8 measurements was then calculated, and that was the resulting value for the thickness of the layer for each sample.

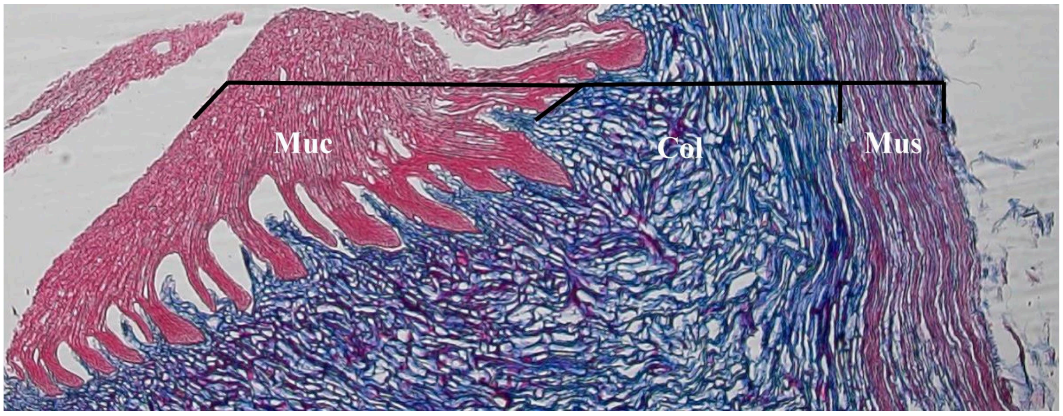

Figure 10. Vaginal tissue composition, transverse section (5x), stained with Masson's Trichrome. Muc = Mucosa; Col = Collagen layer; Mus = muscularis.

Tissue density of the vaginal tissue was also measured. I measured this through converting images to a RGB stack. Then, the resulting black and white images' thresholds were changed until the collagen fibers were in contrast. Image J was then used to count the area of the collagen fibers in the photo, as seen below in Figure 11. The vaginal collagen density was calculated to equal the total area of white fibers divided by the standard cropped area of the photo.

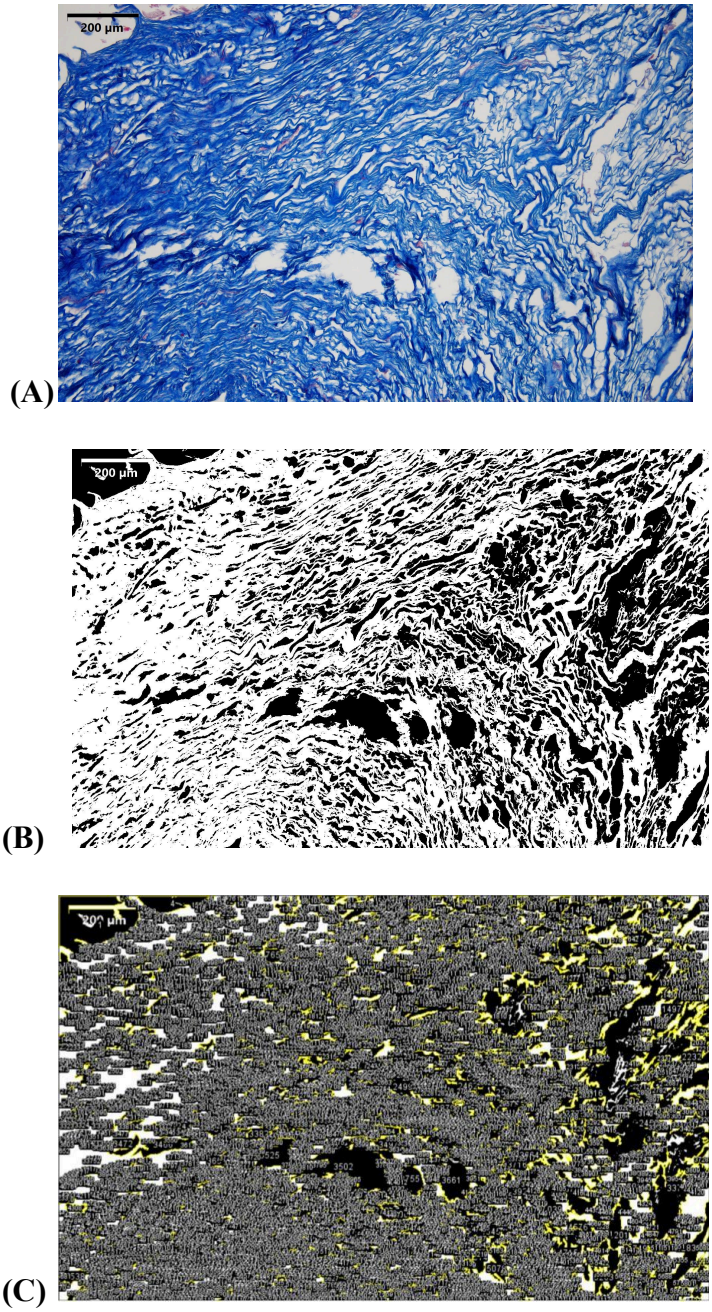

Figure 11. Example of vaginal tissue density measurement. (A) Original photo of vaginal tissue; (B) One of the three RGB stacked black-and-white photos with adjusted threshold; (C) Picture after analyzing area of collagen particles in Image J

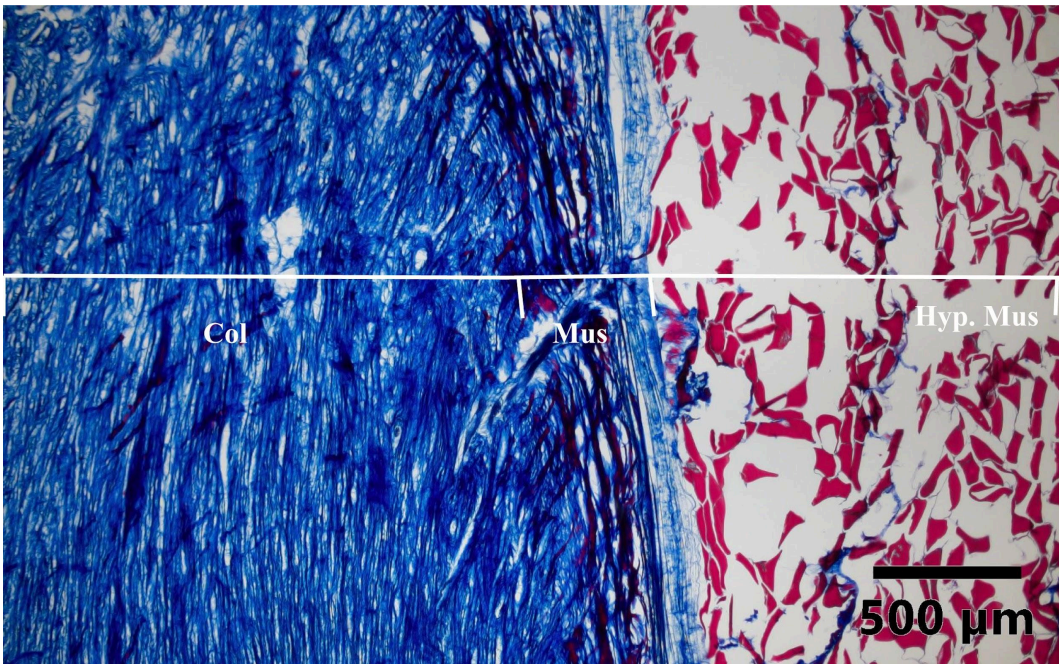

Figure 12. Anal pad composition, transverse section (5x), stained with Masson's Trichrome. Col = Collagen layer; Mus = smooth muscularis; Hyp. Mus = Hypaxial muscle.

For the anal pads, the collagenous and smooth muscle layers were measured (Figure 12). The thickness of the layer was measured using either Feret's diameter or minimum in Image J. Each slice of the pad's layers were measured at 3 different points: the maximum length of the left and right lateral sides of the pad, and the minimum length at the divet in the middle of the pad. These 3 measurements were then averaged to get the average thickness of the pad's layers in that slide. All of the average thicknesses of the individual slides were then averaged to get the overall average thickness of each pad.

Pectoral fin histology

Pectoral fin tissues from females and males were prepared for histology. A hard tissue blade was used to slice samples, but the tissues were too friable, particularly in females, so it was difficult to get whole slices from them. Nevertheless, I measured the epidermal layer thickness of a few specimens that had partially complete pectoral fin skin cover, specifically HYCO107F, HYCO102F, HYCO110M, and HYCO112M. I measured the thickness using Image J and Feret's diameter measurements, in order to determine whether pectoral fin thickness differed in males and females.

Analysis of anal pad and vaginal tissue composition

Google sheets software was used to calculate the average thickness and density of the layers within the vaginal tissue and the anal pad tissue. Given the low sample size of the vaginal samples, statistical analysis was not conducted. Instead, bar graphs of vaginal layer thickness and vaginal collagen density were created, in order to visualize the trends.

As the sample size for anal pads was low, we could not conduct statistical analysis on the data. To show the significant difference between adult female and male ratfish anal pad tissue composition, a bar graph was created in Google Sheets. All bar graphs were then edited using Adobe Illustrator.

RESULTS

Anatomical findings

During dissection of the ratfish specimens, some interesting observations were made. When dissecting juveniles, I found that some juveniles had what appeared to be only one vaginal opening. When dissecting further and attempting to make a mold, I discovered that while the juvenile ratfish had only one opening to the outside, it did have the paired vaginal openings further inside the vaginal canal. This showed the development of the vaginal openings as ratfish pass through stages of ontogeny (juvenile vs adult). As we can see below in the 3D scan of a juvenile ratfish vagina mold (Fig. 13b), there is one hole at the base, and then it bifurcates into two separated paired vaginas. The difference in size between the two vaginal canals depicts that this vagina was still developing in its juvenile stage.

(A) Juvenile ratfish with two vaginal openings

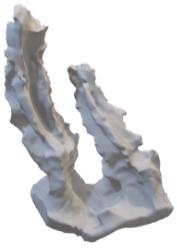

(B) 3D juvenile ratfish vagina silicone model

(C) Juvenile ratfish with one vaginal opening

Figure 13. Juvenile Ratfish anatomy.

In the adult female ratfish, as pictured below in Figure 14b, there are two clear vaginal openings, and the vagina is completely bifurcated, as shown by the model (14a). In addition, the adult vaginas tended to have a lot of folds, while the juvenile vaginas were a lot more smooth. These folds can be seen depicted in the models.

(A) Adult ratfish vagina model

(B) Paired vaginal openings in Adult ratfish

Figure 14. Adult ratfish vagina anatomy

3D Analysis Results

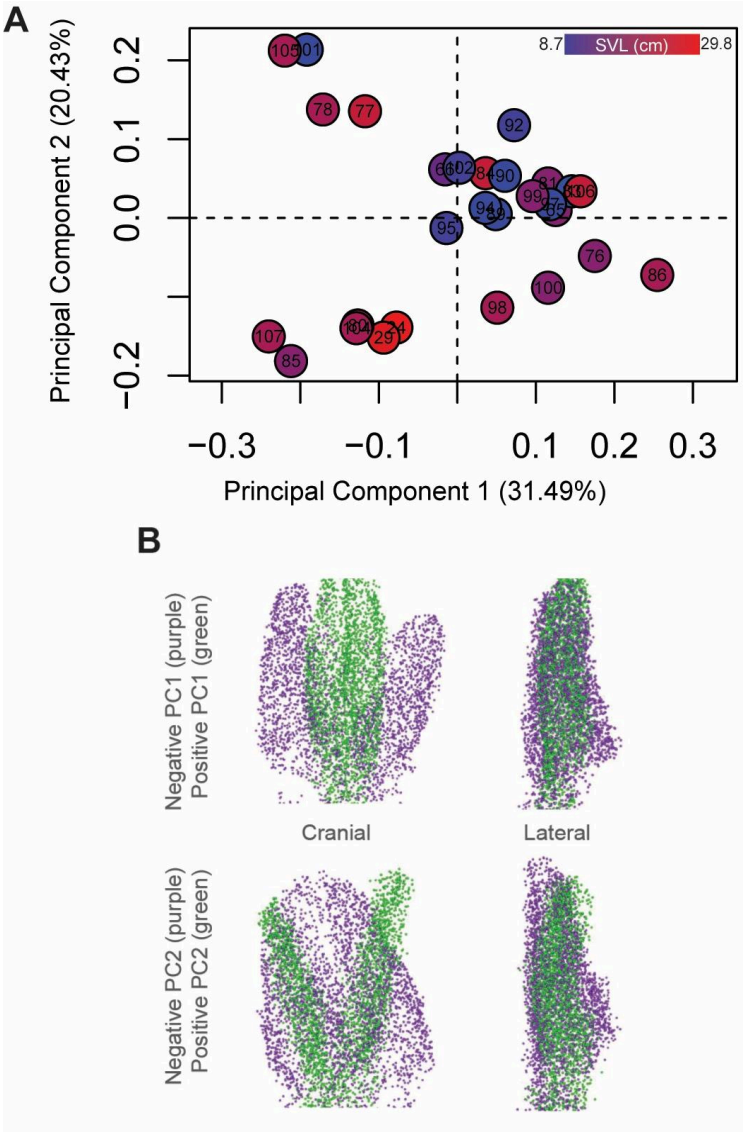

Figure 15. Principal component analysis of 2000 landmarks showing variation of vaginal shape along Principal Component 1 and Principal Component 2. Key: Red = Larger SVL, Blue = smaller SVL. Each point represents one specimen, with its corresponding ID number. (B) Point clouds showing changes in vaginal shape with respect to the positive and negative ends of PC1 (top) and PC2 (bottom).

Figure 15a. shows the results of the principal component analysis. The points each represent one specimen. Points that are red indicate a larger SVL, whereas the blue points indicate a smaller SVL. Principal component 1 accounted for 31.49% of the variation in vaginal shape, whereas principal component 2 accounted for 20.43%. The other principal components (3-27) , were less than 10% of total variation, so they are not analyzed further.

Figure 15b. depicts point clouds summarizing the positive and negative ends of principal component 1 (top) and principal component 2 (bottom). Each point cloud image consisted of two point clouds (one green and one purple) superimposed upon each other. The purple point cloud indicated the negative end of its corresponding principal component, whereas the green point cloud represented the positive end of the corresponding principal component.

The negative end of principal component 1 depicted a widely bifurcated vaginal shape, as well as individually wider vaginal canals. The negative principal component 2 showed a narrower bifurcated vaginal shape with thick vaginal canals. The positive principal component 1 showed a narrow bifurcated vaginal shape, with thin vaginal canals, while the positive principal component 2 depicted a wider bifurcated shape also with thin vaginal canals. Positive principal components had thinner vaginal canals than negative principal components (PC1 and PC2, purple).

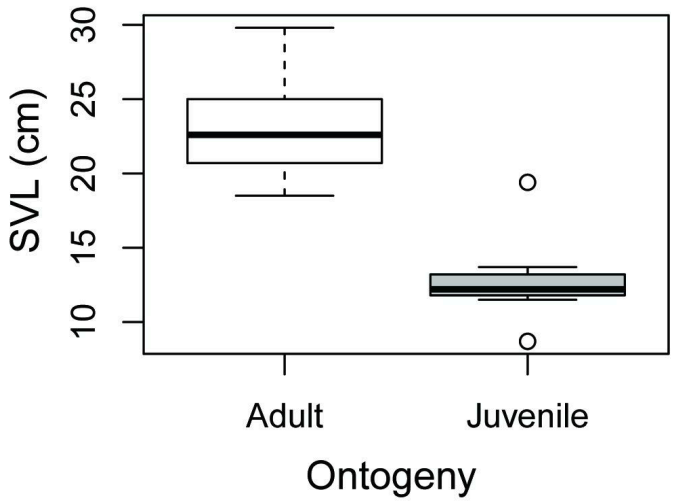

Figure 16. Box plot showing difference in SVL between ontogeny of females (juvenile vs adult)

As shown in Figure 16, there is a difference in the snout-vent length as the female ratfish grow from juveniles to adults. Adult females on average have an average SVL of 22.93 cm and juvenile females on average have an SVL of 12.67 cm. However, there was one female (HYCO081J) with a large SVL that was classified as a juvenile.

All Vaginas ANOVA		
	R^2	p
SVL	0.075	0.037
Ontogeny	0.025	0.697

Table 2. Results of the ANOVA from AUTO 3DGM analysis analyzing the significance of SVL and Ontogeny on the shape of female vaginal pouch shape

Our analysis showed that there is a significant relationship between vaginal shape and SVL, as p is less than 0.05%. Therefore, larger females had different vaginal shapes from smaller females. However, there is not a significant relationship between vaginal shape and ontogeny, as the p value was 0.697, so we could not conclude that adult females had different vaginal shapes than juveniles.

Histology results

Vaginal tissue examination

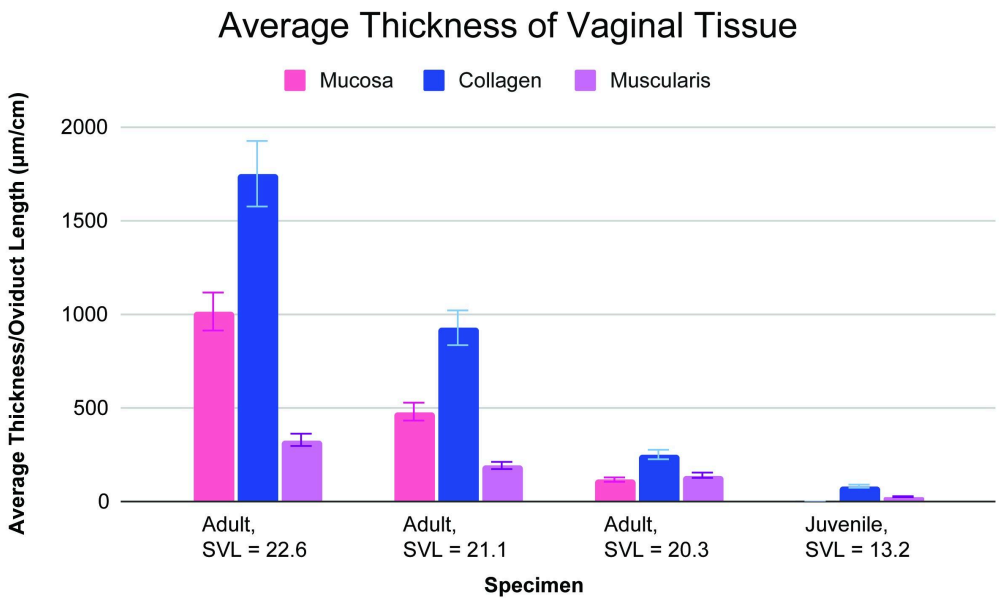

Figure 17. Average Thickness of Vaginal Tissue.

Figure 17 depicts the average thickness of the 3 layers of the vaginal tissue: mucosa, collagen layer, and muscularis. Average thickness was divided by corresponding oviduct length, in order to standardize the measurement. The average thickness of all layers was largest in HYCO107F, the female with the

largest SVL. The juvenile had no mucosa, and the smallest amount of collagen and muscularis. While statistical analysis could not be conducted due to low sample size, the average thickness of each layer increased with a larger SVL across all specimens. The variation of average thickness of vaginal tissue across adults shows that as body size increases, the thickness of vaginal tissue increases, according to the data collected.

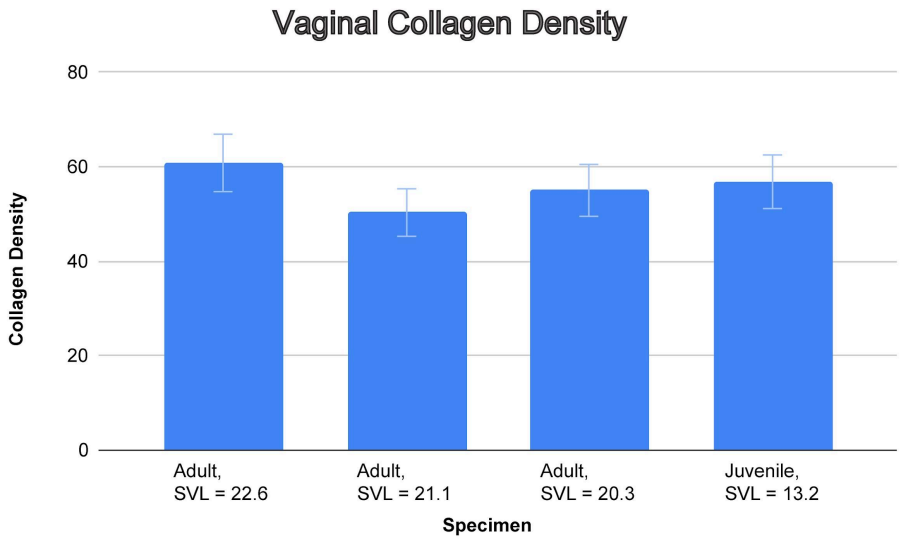

Figure 18. Average Vaginal Collagen Density

The average vaginal collagen density was the largest at 60.8% in HYCO107A, which was the largest female. For HYCO085A, the density was 54.9% and for HYCO100A the collagen density was 50.32%. The juvenile ratfish, HYCO102J, had a collagen density of 56.82%. While our small sample size prevented us from statistically analyzing these patterns, it is apparent that there were no large differences in collagen density between the individuals we sampled.

All histological vaginal measurements were recorded in Tables 11-13, Appendix C.

The adult female vaginal pouch slides indicated the presence of 3 layers: mucosa, a collagen layer, and smooth muscle (muscularis). The mucosa stained light pink and was characterized by deep folds loosely attached to the collagen layer, whereas the collagen layer stained bright blue and was characterized by seemingly short collagen fibers running in a circumferential direction around the vagina. The smooth muscle layer was characterized by a parallel fiber pattern and stained light purple or blue with red specks. Figure 19 below depicts the vaginal layers.

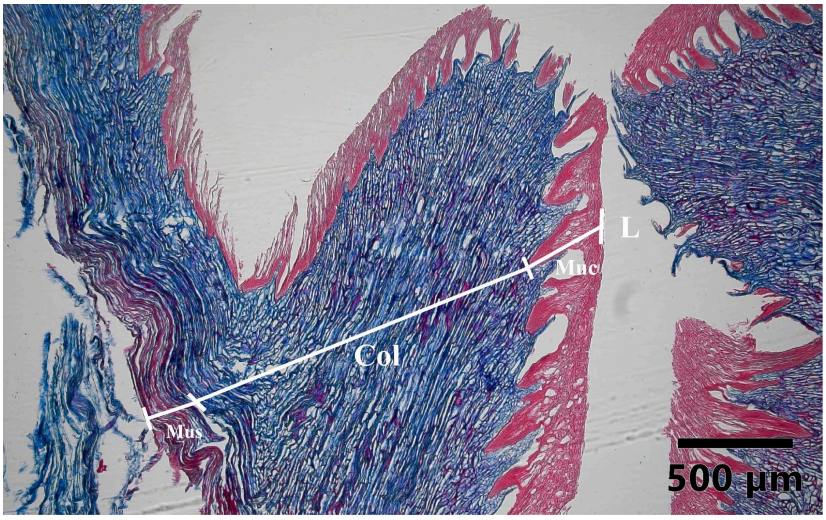

Figure 19. Transverse slice of vaginal tissue stained with Masson's Trichrome, photographed at 5x. Muc=Mucosa, Col = collagen layer, Mus= muscularis, L = lumen.

In the sagittal vaginal pouch slides of the adult female HYCO107F, the largest reproductive female that had 2 eggs in the oviduct, the muscularis was

characterized by concentric hot pink muscle fibers, the collagen fibers are also concentric but much less dense than the muscle fibers, as shown below in Figure 20.

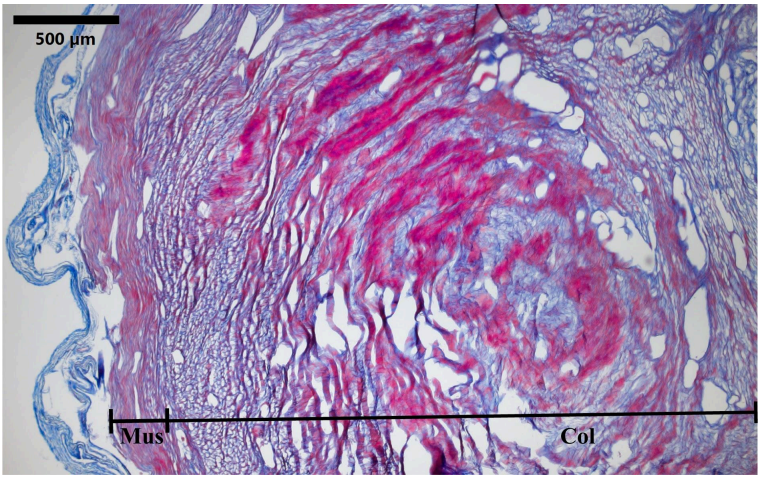

Figure 20. Unique fiber pattern in adult female HYCO107F, sagittally sectioned vagina stained with Masson's Trichrome, photographed at 5x.

In the juvenile vagina, only the collagen layer and smooth muscle layer, as well as some striated muscle were found. There is no mucosal layer present in the juvenile, and instead the lumen is right in the middle, as shown below in Figure 21.

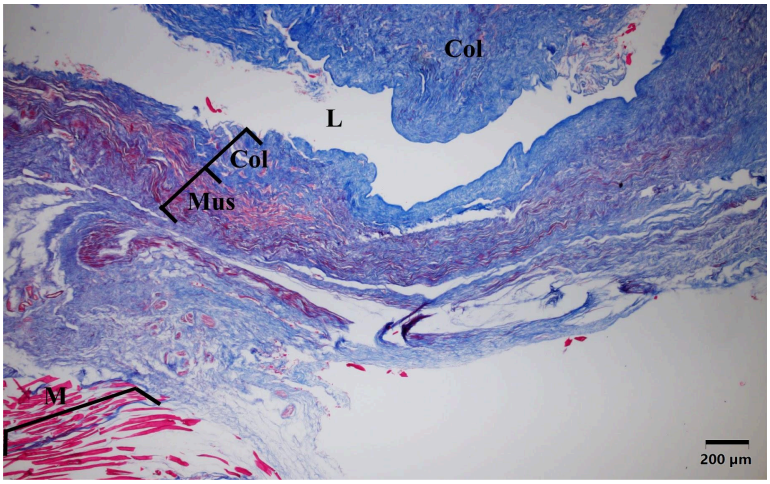

Figure 21. Juvenile vagina stained with Masson's Trichrome, photographed at 5x. L=lumen, Col = collagen layer, Mus = smooth muscularis, M = striated muscle

When preparing the samples for histology, a pink-colored tissue was found in the reproductive tract of one of the medium-sized females (HYCO100F). As shown in Figure 22, this tissue is stained blue, which indicates that it is collagenous.

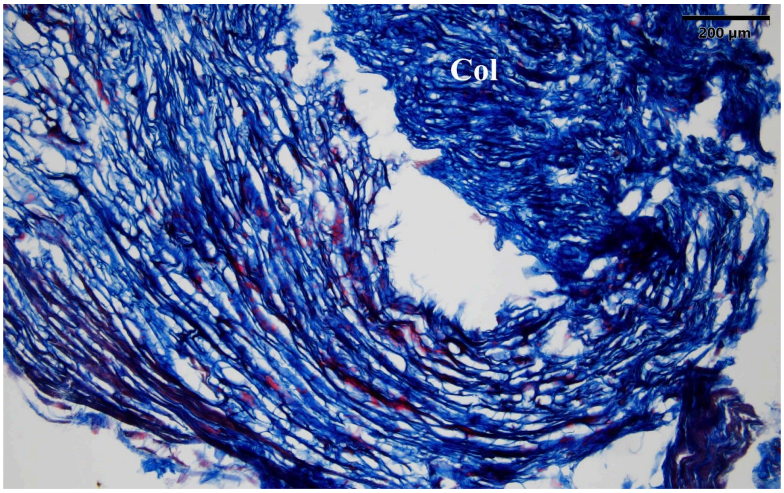

Figure 22. Pink-colored vaginal tissue (10x), stained with Masson's Trichrome, showing collagenous tissue. Col = Collagen

An elastin stain was conducted on 5 slides, in order to determine if elastin was present in the anal pad, vaginal, or fin tissue. Elastin is a type of connective tissue that can help tissues recover their shape after deformation, so we thought there could be some in the vaginal wall. However, no elastin was found in any of the tissues, as seen below in Figure 23. As a control, slices were ran of alpaca clitoris tissue where elastin was positive so we know that the stain itself was working.

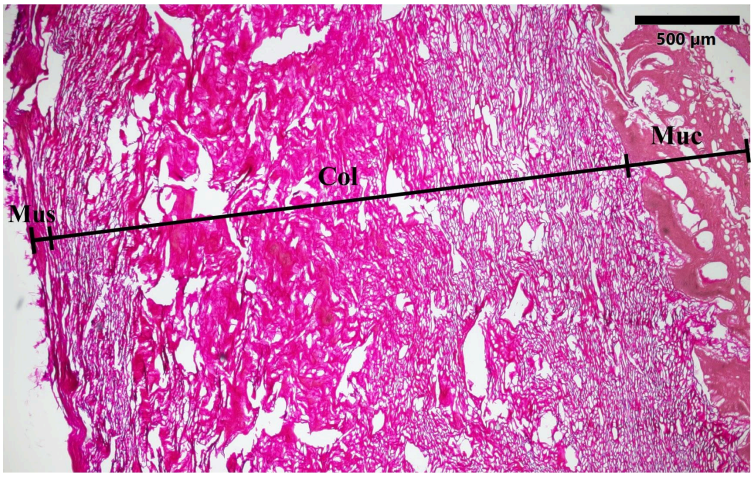

Figure 23. Sagittal vaginal tissue (5x) stained with Elastin Stain showing no evidence of elastin in the tissue.

Anal pad composition

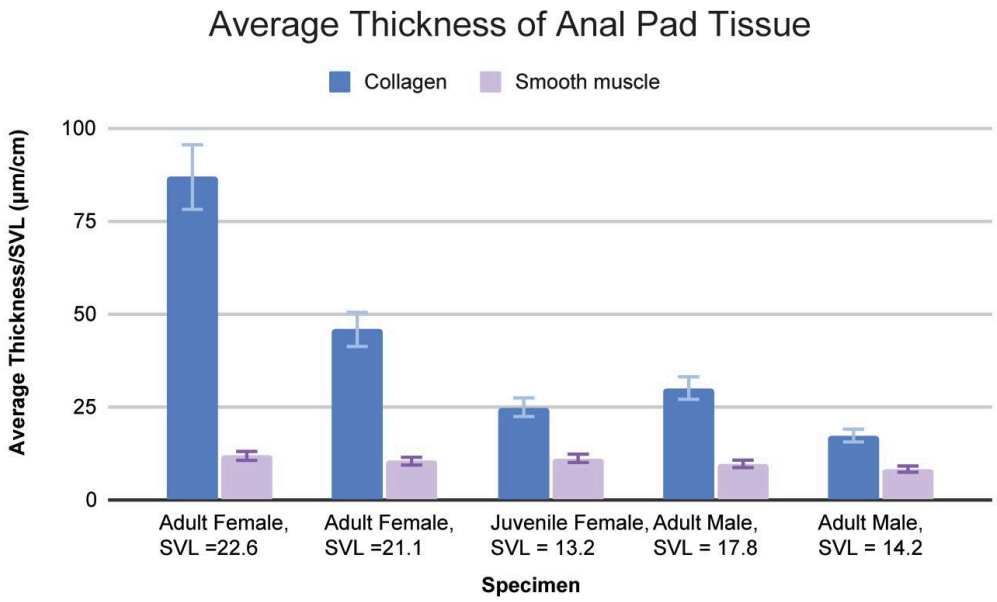

Figure 24. Average Thickness of Anal Pad Tissue

The measurements of microanatomy of the anal pads can be found in Tables 14-15, Appendix C. As the sample size is too small and not independent, this anal pad data was not used for statistical analysis. Instead, we compared the thickness of the anal pad layers in females and males. In order to standardize this data, the average thickness was divided by the SVL of each specimen. In females, the overall average thickness of the collagen layer was 1086.28 micrometers, whereas in males the overall average thickness was 390.58 micrometers. The muscularis thickness appeared to not vary (Figure 24).

Anal pad slides indicated the presence of a collagenous layer, and a smooth muscle layer on top of the striated muscle of the hypaxial musculature of the fish as shown in the Masson's Trichrome-stained slides, the collagen layer

stained blue, whereas the smooth muscle layer stained dark pink/red and was fibrous. The hypaxial muscle layer is characterized by hot pink muscle fascicles. In females, the presence of these 3 layers of the anal pad were very clear; as indicated below in Figure 25. In males, the 3 layers were present but in very small levels, thus showing that there is not a well developed anal pad present in males (Figure 26).

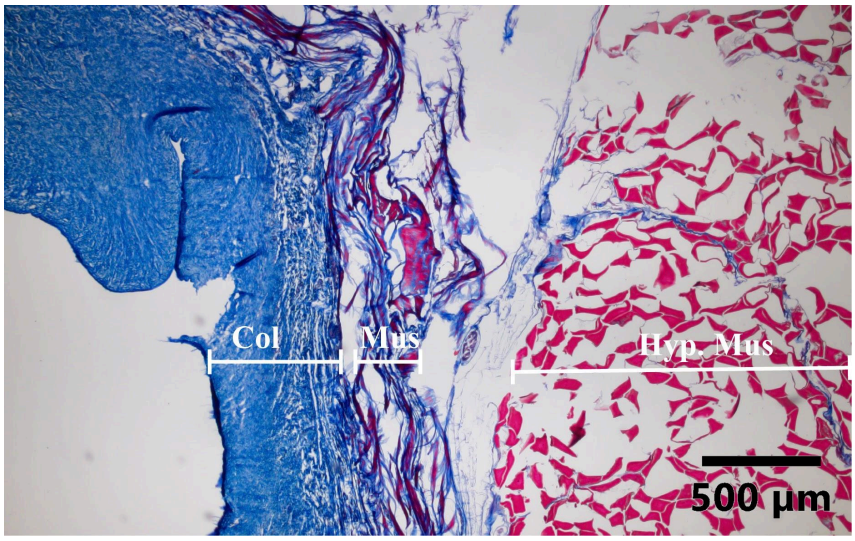

Figure 25. Adult Female anal pad composition. HYCO107FPad2 stained with Masson's Trichrome and photographed at 5x, showing a thick collagenous layer above the hypaxial musculature. Col = Collagen, Mus=Muscularis, Hyp. Mus=Hypaxial musculature.

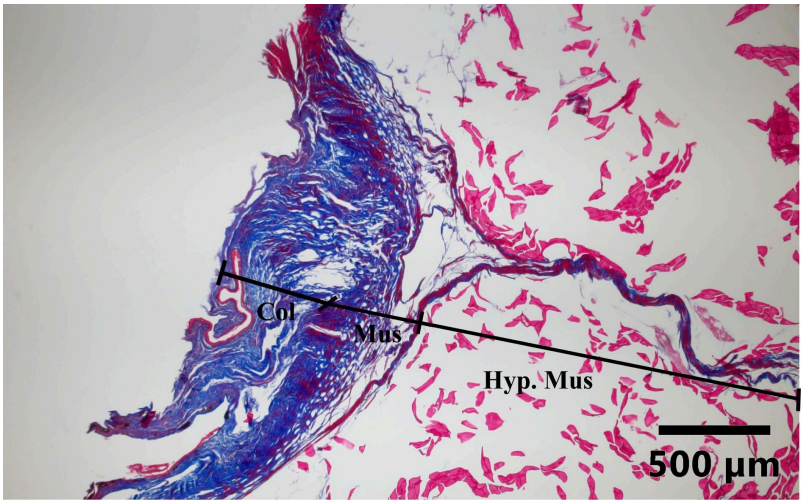

Figure 26. Adult male tissue composition at anal "pad" location, showing that males do not have well developed pads. Col = Collagen, Mus=Muscularis, Hyp. Mus=Hypaxial musculature.

In the larger females, different patterns of collagen fiber arrangement were observed in the blue collagen layer, as pictured in Figure 27. The ventral outermost collagen layer was composed of a blue layer with several vacuoles. The next section of the collagen layer had a radial arrangement of collagen fibers, radiating from the deep midpoint of the anal pad out towards the right and left sides of the fish, so that the central collagen bundles were vertically oriented, but as they moved laterally, they became horizontally arranged and looked almost parallel to each other. The smooth muscle layer was arranged in a circumferential direction right below the collagen.

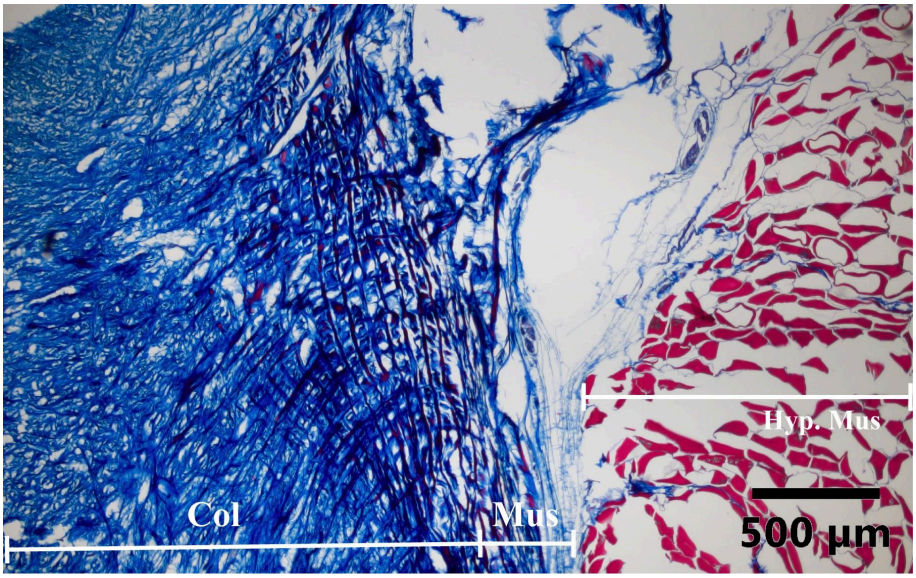

Figure 27. Variety of collagenous patterns in HYCO107FPad3, stained with Masson's Trichrome, photographed at 5x. Col=Collagen, Mus =Muscularis, Hyp. Mus =Hypaxial musculature

Another observation regarding the anal pad composition is that in the juvenile female anal pad, as well as in the male samples, there were vertical lines of collagenous fibers within the muscularis region. This pattern is pictured below in Figure 28. The presence of this pattern in both sexes could be due to the juvenile female still developing its anal pad, and the male not having a developed anal pad. This pattern could be indicative of typical non-anal pad tissue.

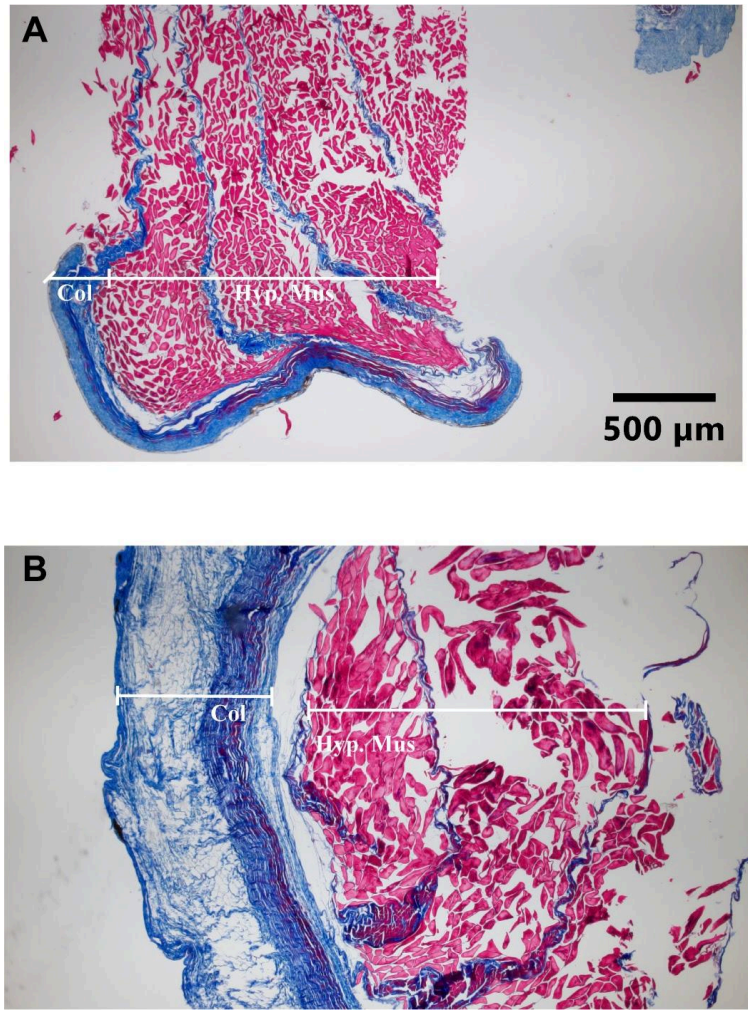

Figure 28. Similar collagen pattern in female juvenile and males (A) Pattern present in juvenile female anal pad striated muscle region (B) Similar pattern present in male anal striated muscle tissue. Col = Collagen, Hyp. Mus=Hypaxial musculature

Pectoral fin thickness

Specimen ID	**Sex**	**Ontogeny**	**Average Epidermal Layer Thickness (µm)**
HYCO107F	Female	Adult	181.359
HYCO102F	Female	Juvenile	188.14
HYCO110M	Male	Adult	230.156
HYCO112M	Male	Adult	148.68

Table 3. List of *H. colliei* pectoral fin samples in histological study with average measurements of epidermal layer thickness

Table 3 shows the average thickness of the epidermal layer of the pectoral fin of 2 females and 2 males. The complete measurements of the epidermal layer of the pectoral fin of males and females can be found in Table 16, Appendix C. From my measurements it appeared as though contrary to my expectation, the males have thicker skin in the pectoral fins than the females. Unfortunately the female fin samples were torn during slicing, so it is not clear if these measurements are complete. Figure 29 illustrates the condition of the pectoral fin samples.

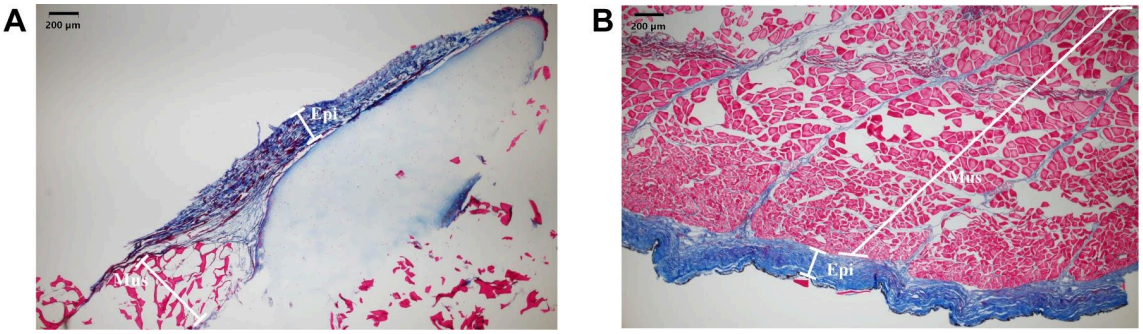

Figure 29. Transverse section of female and pectoral fins stained with Masson's Trichrome, photographed at 5x. Epi = Epidermis, Mus = Muscle (A) Transverse section of female pectoral fin, showing torn tissue (B) Transverse section of male pectoral fin, showing slightly more intact tissue

DISCUSSION

The female genital morphology of the ratfish had not been described so far, and here I have made several observations that increase our knowledge of these structures. At the macroscale, larger females have lots of folds in the walls of their vaginal canals, suggesting that they can stretch during mating and oviposition, both of which are important functions of the vagina. On the other hand, juvenile vaginas do not have folds suggesting a limited ability to stretch.

Shape of vaginal pouches

I found that size is associated with vaginal shape in female ratfish, where larger females had wider vaginal canals that were less widely bifurcated. Wider canals would probably be associated with the ability to mate, since the males have inflatable claspers that would require a wider canal to fit in. Other studies such as Lara Granados et al., 2022 have found that svl (body size) is associated with genital shape, so this finding is expected if coevolution is occurring between males and females. The ontogeny, however, was not significantly associated with genital shape, as the p value was above 0.05. Regarding the variation of all the vaginal shapes, principal component one accounted for 31.49% of variation and principal component 2 accounted for 20.43%. As the vaginal shapes in the ratfish

were extremely diverse, this study adds to evidence from previous studies that show high vaginal shape variance (Orbach et al., 2018; Hedrick et al., 2019).

Vaginal tissue composition

As the thickness of the vagina is a larger value when the females are a larger size, it could be hypothesized that they develop a thicker tissue due to copulation, or in adaptation to the spines on the male ratfish's claspers. However, as the sample size was too low, we cannot make any conclusive statements. Orr *et al.* (2022) found that in bats, vaginal thickness has coevolved with the presence of penile spines. Ratfish vaginal tissue evolving with the presence of spines on the male's paired claspers would be an example of antagonistic coevolution, as the males' spines would cause harm and then lead to the counteradaptation of evolved thicker vaginal tissue. This form of coevolution has been studied before in seed beetles. Male seed beetles have genital spines that were found to cause more harm to females during copulation, and the females in response adapted to have a larger proportion of connective tissue in their reproductive tract (Rönn et al., 2007).

The density of the collagen in the vaginas was not obviously different. As male ratfish have spines on their claspers, these spines could pierce the vaginal tissue, thus as a result over time the adult female ratfish would have less dense vaginal collagen. Again, additional testing would need to be done with a larger sample size for further research and statistical analysis to support this. Additionally, evidence has been found in bats that vaginal collagen density does

not appear to covary with any male features (Orr et al., 2022). Thus, it appears our results add on to evidence that vaginal density is not affected in conjunction with male features.

Anal pad composition

The anal pad tissue was found to be highly collagenous. The collagen thickness in anal pads appeared to increase with size of the female ratfish. In male ratfish, the collagen thickness was lower, as males lack an anal pad. In addition, the fibers in adult females vary in patterns. For example, the uppermost collagen layer had vacuoles in its collagen. This composition seemed to provide more cushioning for adult females, given the highly collagenous nature of the tissue. It could be that the adult females could use the anal pad as a cushion during female-specific behavior-related activities, such as spawning. The anal pad could function to provide support to the adult females when they are depositing the egg cases in the muddy ocean floor. As the egg remains attached to the female for 24 hours, I think that the function of the anal pad as a cushion would be to attach to either the ocean floor or an object near it, in order to provide support when spawning (Berrio et al., 2023). Thus, the anal pad being most prominent in larger females could be due to a reproductive reason.

Pectoral fins

Despite previous findings that female sharks have a thicker epidermis than males (Crooks et al., 2013), the ratfish females do not seem to have an obviously thicker epidermal layer in their pectoral fins. However, this could be an artifact of the technical difficulties in obtaining good slides for the females compared to the males, but it could also indicate that female ratfish may not have adapted the tissue of their pectoral fins to the spiny attachment of the male's claspers.

APPENDIX

Appendix A

Table 4. Measurements of macroanatomy of all dissected female specimens

Specimen ID	Ontogeny	SVL (cm)	Length 2 (cm)	Oviduct Length (mm)		Largest Egg Diameter (mm)	Anal Pad Length (mm)	Anal Pad Width (mm)
				Right	Left			
HYCO029F	adult	27.2	24.5	90	105	1.31	ND	ND
HYCO024F	adult	29.8	27.2	87.2	86.4	0.37	ND	ND
HYCO065F	adult	20.5	47.2	74.3	83.7	1.8	ND	ND
HYCO066F	adult	18.5	42	83.8	77.8	<1	ND	ND
HYCO0076F	adult	20.7	24.8	97	88	7	33.8	8.9
HYCO0077F	adult	25.4	24.1	127	122	5.5	ND	ND
HYCO078F	adult	22.2	22.9	68.6	69.5	3.5	37.6	10.8
HYCO079F	adult	17.5	21.3	77.4	80.3	n/a	ND	ND
HYCO080F	adult	22.6	23.4	68.1	70	7.1	34.1	11.3
HYCO081F	juvenile	19.4	26.5	83	66.2	1.6	29.6	8.9
HYCO082F	juvenile	13.4	21.1	54.9	56.9	1	30	7.7
HYCO083F	juvenile	8.7	27.8	34.8	30.9	n/a	23.7	7.8
HYCO084F	adult	25	28.5	72.1	71.8	2.3	33.7	11.3
HYCO085F	adult	20.3	24.6	83.4	85.8	1.3	11.92	12.6
HYCO086F	adult	23.2	28.8	66.7	63.3	5.9	ND	ND
HYCO087F	juvenile	11.8	19.6	51.3	53.8	n/a	25.4	9.8
HYCO088F	juvenile	13.5	21	54	49.2	n/a	30.8	10
HYCO089F	juvenile	12.5	20.8	53.9	56	n/a	33.3	10.4
HYCO090F	juvenile	11.9	18.7	45.5	48.3	n/a	26	10.2
HYCO091F	juvenile	10.4	18	ND	ND	n/a	25.4	6.4
HYCO0092F	juvenile	13.1	17.1	62.1	53	n/a	34.9	10
HYCOO93F	juvenile	11.6	21.5	58.5	48.6	<1	ND	ND

HYCO094F	juvenile	11.8	18.6	45	49.3	<1	30.7	9.3
HYCOO95F	juvenile	13.7	31	57.4	59	<1	41.8	8.5
HYCOO96F	juvenile	12.7	31.1	ND	ND	ND	46.2	11.4
HYCOO97F	juvenile	11.8	28.7	ND	ND	ND	31.5	8.8
HYCOO98F	adult	21.7	48.8	90.5	94	6.8	46.3	16.2
HYCOO99F	adult	20.5	26	99.6	100.6	1.8	40.6	9.9
HYCO100F	adult	21.1	25.7	86.6	84.9	3.6	26.4	14.9
HYCO101F	juvenile	11.5	16.9	55.1	48.6	n/a	28.4	9
HYCO102F	juvenile	13.22	20.5	60.2	57.7	n/a	11.6	11.5
HYCO103F	juvenile	13.8	21.3	66.7	67.2	ND	38.6	10
HYCO104F	adult	23	22.5	99	96.8	5	44.6	12.1
HYCO105F	adult	23.4	22.5	89.4	76.3	5.95	39.1	16.2
HYCO106F	adult	25.1	25.5	64.1	59.1	26	ND	ND
HYCO107F	adult	22.6	19.1	80.3	68.2	6.4	57.6	18.6

Table 5. Measurements of macroanatomy of all dissected male specimens

Specimen ID	**Ontogeny**	**SVL (cm)**	**Length 2 (cm)**	**Anal Pad Length (mm)**	**Anal Pad Width (mm)**
HYCO110M	Adult	17.8	23.4	21.9	13.5
HYCO111M	Adult	18.2	23.4	37.8	11.6
HYCO112M	Adult	14.2	23.3	31	13.2

Table 6. List of *H. colliei* anal pad samples with preservation condition and measurements

Specimen ID	**Preserved in**	**Length (mm)**	**Width (mm)**
HYCO107F	10% formalin	57.6	18.6
HYCO102F	10% formalin	11.6	11.5
HYCO100F	10% formalin	26.4	14.9
HYCO110M	10% formalin	21.9	13.5
HYCO111M	10% formalin	37.8	11.6
HYCO112M	10% formalin	31	13.2

Appendix B

Table 7. Protocol used for processing formalin-preserved specimen

Procedure	**Chemicals**	**Time**	**Temperature (°C)**
Dehydration I	70% EtOH	1 hr	Room temperature
Dehydration II	95% EtOH	1 hr	Room temperature
Dehydration III	100% EtOH I	1 hr	Room temperature
Dehydration IV	100% EtOH II	1 hr	Room temperature
Dehydration V	100% EtOH III	4 hr/overnight	Room temperature
Clearing I	1:1 Histoclear/EtOH	30 min	Room temperature
Clearing II	100% Histoclear I	30 min	Room temperature
Clearing III	100% Histoclear II	30 min	Room temperature
Clearing IV	1:1 Histoclear/Paraffin	15 min	54
Infiltration I	Paraffin I	30 min	54
Infiltration II	Paraffin II	30 min	54
Infiltration III	Paraffin III	1 hr	54

Table 8. Protocol used for Masson's Trichrome Staining.

Chemicals	**Time**
Histoclear I	5 min
Histoclear II	2 min
100% EtOH	2 min
95% EtOH	2 min
70% EtOH	2 min
50% EtOH	2 min
35% EtOH	2 min
H2O	2 min
Masson A	45 s
dH2O rinse	In sink
Masson B	1.5 min
Masson C	20 s
1% Acetic Acid (aq)	3 min
1:1 Acetic Acid/EtOH	30 s
100% EtOH rinse	twice
Histoclear rinse	twice

Table 9. Protocol used for Hematoxylin & Eosin (H&E)

Chemicals	**Time**
Histoclear (I)	5 min
Histoclear (II)	2 min
100% EtOH	2 min
95% EtOH	2 min
70% EtOH	2 min
50% EtOH	2 min
35% EtOH	2 min
H2O	2 min
Hematoxylin	1 min 10 s
dH2O rinse	x1
35% EtOH	2 min
50% EtOH	2 min
70% EtOH	2 min
95% EtOH	2 min
Eosin Y	3 min
95% EtOH	2 min
100% EtOH I	2 min
100% EtOH II	2 min
100% Histoclear I	5 min
100% Histoclear II	5 min

Table 10. Protocol used for Elastin Staining

Chemicals	**Time**
Histoclear I	5 min
Histoclear II	2 min
100% EtOH	2 min
95% EtOH	2 min
70% EtOH	2 min
50% EtOH	2 min
35% EtOH	2 min
H2O	2 min
Verhoeff's solution	1 hr
dH2O rinse	x2-3
2% ferric chloride	1-2 min
dH2O rinse	x3
Solution D	1 min
Running tap water	5 min
Counterstain I	3-5 min
95% EtOH	2 min
100% EtOH	2 min
100% EtOH	2 min
100% Histoclear I	3 min
100% Histoclear II	3 min

Appendix C

Table 11. List of *H. colliei* vaginal samples in histological study with average measurements of microanatomy.

Specimen ID	**Ontogeny**	**Average Muscularis Thickness (µm)**	**Average Collagen Thickness (µm)**	**Average Collagen Density % (Transverse)**	**Average Mucosa Thickness (µm)**
HYCO 107F	Adult	329.14	1750.14	60.80	1014.17
HYCO 100F	Adult	192.04	927.48	50.32	479.65
HYCO 085F	Adult	140.15	250.55	54.99	116.47
HYCO 102F	Juvenile	25.49	81.72	56.82	0

Table 12. List of *H. colliei* vaginal samples in histological study with all measurements of vaginal thickness

Specimen ID	**Ontogeny**	**Slide**	**Mucosa Thickness (µm)**	**Collagen layer Thickness (µm)**	**Muscularis Thickness (µm)**
HYCO107F	Adult	HYCO107 VPB	1078.677	580.315	197.651
			891.358	3,314.82	377.908
			0	699.159	225.123
			0	2,248.34	326.62

			1917.031	898.412	561.61
			0	1354.308	626.287
			723.842	489.939	434.7
			0	2279.841	1038.416
		HYCO107 VPC	1251.023	1306.538	373.324
			1123.292	2955.702	356.955
			1528.913	548.626	502.633
			1146.84	2298.12	491.301
			1206.126	804.577	353.971
			1829.181	1404.752	148.385
			2191.413	1219.368	146.003
			1069.628	2973.627	169.675
		HYCO107 VPD	1243.559	745.028	190.318
			98.274	2679.211	154.327
			790.89	705.979	204.342
			98.977	3420.806	197.375
			655.536	776.545	191.018
			346.839	2724.097	209.867
			301.014	2666.772	132.268
			236.763	2908.594	289.187

			272.575	570.602	173.944
			239.015	487.149	135.237
			0	1030.785	312.106
			326.416	699.525	209.272
			130.367	477.9	143.099
		HYCO100	103.499	487.601	366.593
		VPA	166.237	799.562	150.884
			575.961	309.512	294.775
			157.595	400.736	202.372
			249.242	475.863	443.05
			569.26	737.545	349.061
			132.792	2000.327	210.288
			446.962	369.392	169.624
		HYCO100	359.37	312.788	151.022
		VPB	451.808	757.035	193.812
			813.814	0	0
			403.509	450.405	205.146
			598.832	751.795	253.813
			483.659	1628.124	202.578
			704.068	348.43	251.672
		HYCO100			
HYCO100F	Adult	VPB	346.374	2010.225	437.68

			315.817	458.343	104.183
			697.934	0	0
		HYCO100 VPC	0	508.822	148.705
			912.046	626.121	319.264
			0	877.893	99.372
			765.012	2061.193	103.843
			0	806.458	201.372
			1738.968	798.065	85.099
			0	754.479	75.092
			1451.289	1233.993	104.11
		HYCO100 VPC	0	1747.138	127.632
			235.171	738.827	0
			354.035	2131.241	92.628
			350.677	2364.545	100.746
			387.346	1882.338	24.276
			339.204	2148.211	65.094
			419.324	106.801	0
			259.281	2432.862	128.515
HYCO085F	Adult	HYCO085 VPC	0	566.191	181.071
			155.29	176.58	117.159
			0	190.69	159.678

			0	179.923	128.037
			0	684.266	63.524
			95.576	159.851	122.733
			0	256.532	133.829
			0	111.524	145.029
			0	457.248	194.2
			226.468	215.741	104.089
		HYCO085 VPC	0	845.406	269.971
			78.772	238.708	227.981
			0	341.381	164.012
			0	158.386	86.785
			0	283.626	182.847
			92.024	176.322	86.523
			0	603.159	133.545
			0	151.473	95.955
			0	449.876	167.328
			0	220.981	92.318
		HYCO085 VPD	0	306.1	131.121
			0	153.386	98.266
			0	190.154	104.368
			0	153.522	87.785

			0	105.276	104.484
			0	154.231	94.236
			0	215.889	119.107
			0	223.449	106.145
			0	230.957	119.107
			0	168.627	134.202
		HYCO085 VPD	110.682	115.804	91.929
			0	279.032	65.85
			0	248.071	118.231
			0	99.108	103.485
			0	67.101	73.881
			0	108.708	53.681
			0	235.405	58.26
			0	147.762	68.328
			0	149.811	90.025
			0	201.852	124.231
HYCO102F	Juvenile	HYCO102 VP	0	372.535	92.849
			0	659.404	0
			0	673.755	0
			0	261.764	165.286
			0	845.298	274.455

			0	463.57	112.511
			0	548.682	133.863
			0	220.989	119.759
			0	293.338	154.36

Table 13. List of *H. colliei* vaginal samples in histological study with all measurements of vaginal collagen layer density

Specimen ID	**Ontogeny**	**Slide**	**Collagen Area (µm^2)**	**Total Area (µm^2)**	**Density %**
HYCO107F	Adult	HYCO107 VPB	11085.0999	16401.9249	67.58
		HYCO107 VPC	9823.2909	16401.9249	59.89
		HYCO107 VPD	9011.0819	16401.9249	54.94
HYCO100F	Adult	HYCO100 VPB	9533.8929	16401.9249	58.13
		HYCO100 VPB	8677.7569	16401.9249	52.91
		HYCO100 VPC	7400.4449	16401.9249	45.12
HYCO085F	Adult	HYCO085 VPC	8489.9929	16401.9249	51.76
		HYCO085 VPC	9302.2019	16401.9249	56.71
		HYCO085 VPD	8183.3689	16401.9249	49.89
		HYCO085 VPD	10108.3819	16401.9249	61.63

HYCO102F	Juvenile	HYO102VP	9320.2899	16401.9249	56.82

Table 14. List of *H. colliei* transverse anal pad samples in histological study with average measurements of microanatomy.

Specimen ID	**Sex**	**Ontogeny**	**Average Collagen Thickness (µm)**	**Smooth Muscle Average Thickness (µm)**
HYCO107F	Female	Adult	1962.237944	267.2736667
HYCO100F	Female	Adult	967.5614167	220.0220833
HYCO102F	Female	Juvenile	329.04075	147.7203333
HYCO110M	Male	Adult	535.4283333	172.43783333
HYCO112M	Male	Adult	245.7323333	117.8196667

Table 15. List of *H. colliei* transverse anal pad samples in histological study with all measurements of microanatomy.

Specimen ID	**Sex**	**Ontogeny**	**Slide**	**Collagen layer Thickness (µm)**	**Muscularis Thickness (µm)**
				1490.711	492.351
				465.531	457.356
				1120.041	129.258
				1687.405	266.917
				688.002	344.288
HYCO107F	Female	Adult	HYCO107AP2		

				1834.871	315.961
			HYCO107AP3	2355.715	222.86
				547.491	143.988
				2483.818	178.549
				3449.783	265.936
				1213.775	86.196
				3379.886	359.738
			HYCO107AP4	2849.461	212.667
				851.34	286.234
				2901.038	203.041
				2384.753	260.995
				1295.659	120.617
				2712.547	366.979
			HYCO107AP5	2774.381	424.445
				1039.227	458.706
				2127.663	341.702
				882.884	312.687
				1177.212	204.73
				893.65	360.856
HYCO100F	Female	Adult	HYCO100AP1	1039.507	179.659
				458.549	209.937
				700.942	158.417
				1443.999	288.343
				363.825	379.356
				867.186	182.41
			HYCO100AP2	1753.735	168.715
				660.651	328.855
				1472.716	93.495
				1343.304	121.905
				371.498	219.21
				1134.825	309.963
HYCO102F	Female	Juvenile	HYCO102AP1	426.942	162.133
				603.662	222.354

				145.202	85.272
				503.74	114.355
				260.685	115.083
				66.593	61.002
				249.797	123.293
				377.631	199.888
				446.282	138.948
				340.729	112.411
				306.816	206.441
			HYCO102AP2	220.41	231.464
				655.148	156.637
				1132.722	304.982
				560.454	268.364
				163.308	196.272
			HYCO110MA	700.938	108.372
HYCO110M	Male	Adult	P1	0	0
				103.181	116.453
				662.932	177.972
				170.587	0
				86.503	71.459
			HYCO112MA	361.012	341.034
HYCO112M	Male	Adult	P1	90.179	0

Table 16. List of *H. colliei* pectoral fin samples in histological study with measurements of epidermal layer thickness.

Specimen ID	Sex	Ontogeny	Epidermal layer thickness (µm)
HYCO110M	Male	Adult	215.394
			236.581
			380.816
			163.356
			313.555
			364.072
			91.706
			168.518
			137.405
HYCO112M	Male	Adult	205.062
			170.822
			101.824
			210.227
			55.466
HYCO107F	Female	Adult	254.008
			96.972
			275.02
			45.92
			254.249
			98.705
			347.157
			52.867
			205.707
			182.986
HYCO102F	Female	Juvenile	348.511
			75.233
			225.487
			114.757

			228.654
			81.125
			243.213

Appendix D

```
femaleShape <- read.morphologika("HYCOmorphologika_unscaled.txt")#Load
female shape data
femaleGPA <- gpagen(femaleShape, ProcD = FALSE)

#Run Generalized Procrustes Analysis using bending energy criterion
femaleData <- read.csv("ratfish.csv")

femalePCA <- gm.prcomp(femaleGPA$coords,
                       phy = NULL)
femalePCASum <- summary(femalePCA) #Gives you breakdown of variance and
eigenvalues

#Set a color palette for the PCA based on SVL where larger females are red and
smaller females are blue

pal = colorRampPalette(c("blue", "red"))
femaleGPA$col <- pal(10)[as.numeric(cut(femaleData$SVL,breaks = 10))]

#PCA Plot
femalePCAPlot <- plot(femalePCA,
                      xlab = paste("Principal Component 1 (31.49%)", sep = "",
paste(round(femalePCASum$PC.summary$Comp1[2]*100, digits = 2), sep =
"")),
                      ylab = paste("Principal Component 2 (20.43%)", sep = "",
paste(round(femalePCASum$PC.summary$Comp2[2]*100, digits = 2), sep =
"")),
                    pch = 21,
                     col = "black",
                     bg = femaleGPA$col,
                     cex = 2,
                     cex.lab = 1.2)
text(femalePCAPlot$PC.points[ , 2] ~ femalePCAPlot$PC.points[ , 1],
    labels = femaleData$ID, cex= 0.5, col = c("black"))

# Point cloud figures
procFemale <- procSym(femaleShape)
plot(procFemale$PCscores[,2] ~ procFemale$PCscores[,1])

#Plot at ends of PC1 axes, negative is purple and positive is green, Magnified by
2 to accentuate trends
palette(c("white", "green", "purple"))
posPC1Female <- showPC(2*sd(procFemale$PCscores[,1]),
procFemale$PCs[,1], procFemale$mshape)
```

```
negPC1Female <- showPC(-2*sd(procFemale$PCscores[,1]),
procFemale$PCs[,1], procFemale$mshape)
deformGrid3d(posPC1Female, negPC1Female, ngrid = 0, lines = FALSE)

palette(c("white", "green", "purple"))
posPC2Female <- showPC(2*sd(procFemale$PCscores[,2]),
procFemale$PCs[,2], procFemale$mshape)
negPC2Female <- showPC(-2*sd(procFemale$PCscores[,2]),
procFemale$PCs[,2], procFemale$mshape)
deformGrid3d(posPC2Female, negPC2Female, ngrid = 0, lines = FALSE)

#Make geomorph dataframe
femaleGDF <- geomorph.data.frame(shape = femalePCA$x,
                          svl = log10(femaleData$SVL),
                          coords = femaleGPA$coords,
                         age = femaleData$Age)
#ANOVAs
#Do a Procrustes ANOVA of shape and size for females
femaleFit <- procD.lm(shape ~ svl + ontogeny,
                  data = femaleGDF,
                  iter = 1000)
summary(femaleFit)

#box plot
boxplot(SVL ~ Ontogeny,
       data = femaleData,
       col = c("white", "gray"),
       xlab = "Ontogeny",
       ylab = "SVL (cm)",
       cex.lab = 1.2)
```

LITERATURE CITED

Ah-King, M., Barron, A.B., & Herberstein, M.E. (2014). Genital evolution: Why are females still understudied? *PLoS Biol. 12*(5), e1001851. https://doi.org/10.1371/journal.pbio.1001851

Angulo, A., López,M. I., Bussing, W. A., Murase, A. (2014). Records of chimaeroid fishes (Holocephali: Chimaeriformes) from the Pacific coast of Costa Rica, with the description of a new species of Chimera (Chimaeridae) from the Eastern Pacific Ocean. *Zootaxa*, *3861*(6). https://doi.org/10.11646/zootaxa.3861.6.3

Barnett, L.A.K., Earley, R.L., Ebert, D.A. & Cailliet, G.M. (2009). Maturity, fecundity, and reproductive cycle of the spotted ratfish, *Hydrolagus colliei*. *Mar Biol, 156*(3)**,** 301-316. https://doi.org/10.1007/s00227-008-1084-y

Berio, F., Charron, R., Dagouret, J.-M., De Gasperis, F., Éon, A., Meunier, E., Simonet, M., Verschraegen, N., & Hirel, N. (2023). Husbandry conditions of spotted ratfish (Hydrolagus colliei, Chimaeriformes) in aquaria for Successful embryonic development and long-term survival of juveniles. *Zoo Biology*, *43*(2), 188-198. https://doi.org/10/1002/zoo.21813

Brennan, P.L.R., & Orbach, D.N. (2020). Chapter Three - Copulatory behavior and its relationship to genital morphology. In M. Naguib, L. Barrett, S.D. Healy, J. Podos, L.W. Simmons, M. Zuk (Eds.), *Advances in the Study of Behavior* (Vol. 52, pp. 65-122). Academic Press. https://doi.org/10.1016/bs.asb.2020.01.001

Brennan, P. L. R., & Prum, R. O. (2015). Mechanisms and Evidence of Genital Coevolution: The Roles of Natural Selection, Mate Choice, and Sexual Conflict. Cold Spring Harbor Perspectives in Biology, *7*(7), a017749. https://doi.org/10.1101/cshperspect.a017749

Brennan, P.L. R. (2016). Studying Genital Coevolution to Understand Intromittent Organ Morphology, *Integrative and Comparative Biology*, *56*(4),669–681. https://doi.org/10.1093/icb/icw018

Boyer, D. M., Puente, J., Gladman, J. T., Glynn, C., Mukherjee, S., Yapuncich, G. S., & Daubechies, I. (2015). A new fully automated approach for aligning and comparing shapes. *Anatomical record (Hoboken, N.J. : 2007)*, *298*(1), 249–276. https://doi.org/10.1002/ar.23084

Cailliet, G.M. & Ebert, D.A. (2014). Chapter 1: The Diversity and Natural History of Chondrichthyan Fishes. In Smith, S.L., Sim, R.B., Flajnik, M.F. (Eds.), *Immunobiology of the Shark* (1st ed., pp. 1-28). CRC Press. https://doi.org/10.1201/b17773.

Crooks, N., Babey, L., Haddon, W. J., Love, A. C., & Waring, C. P. (2013). Sexual dimorphisms in the dermal denticles of the lesser-spotted catshark, Scyliorhinus canicula (Linnaeus, 1758). *PloS one*, *8*(10), e76887. https://doi.org/10.1371/journal.pone.0076887

Dean, B. (1906) Chimaeroid Fishes and their development. Carnegie

Institute of Washington.
Didier, D. A. (1995). Phylogenetic systematics of extant chimaeroid fishes (Holocephali, Chimaeroidei). *Novitates American Museum of Natural History* ; 3119, 1-86. https://digitallibrary.amnh.org/handle/2246/3652
Didier, D. A., & Rosenberger, L. J. (2002). The spotted ratfish, Hydrolagus colliei: Notes on its biology with a redescription of the species (Holocephali: Chimaeridae). *California Fish and Game*, *88*(3), 112–125.
Didier, D. A. (2002). Two new species of chimaeroid fishes from the southwestern Pacific Ocean (Holocephali, chimaeridae). *Ichthyological Research, 49*(4), 299-306. https://doi.org/10.1007/s102280200045
Didier, D. A., Kemper, J., & Ebert, D. (2012). Phylogeny, Biology and Classification of Extant Holocephalans. In Carrier, J.C., Musick, J.A., & Heithaus, M.R. (Eds.), *Biology of Sharks and their Relatives* (2nd ed., pp. 97–121). CRC Press. https://doi.org/10.1201/b11867
Hedrick, B. Antalek-Schrag, P. Conith A. J. Natanson, L. J. Brennan, P. L. R. (2019). Variability and asymmetry in the shape of the Spiny Dogfish vagina revealed by 2D and 3D geometric morphometrics. *Journal of Zoology, 308*(1), 16-27. https://doi.org/10.1111/jzo.12653
Johnson, A.G. (1967). Biology of the Ratfish, *Hydrolagus colliei* (Lay and Bennet). [Master's thesis, Oregon State University]. https://ir.library.oregonstate.edu/downloads/6q182p124
Lara Granados, G., Greenwood, J., Secor, S., Shan, S., Hedrick, B. P., Brennan, P.L.R. (2022). Examining the shape and size of female and male genitalia in snakes using three-dimensional geometric morphometrics, *Biological Journal of the Linnean Society*, *136*(3), 466–476. https://doi.org/10.1093/biolinnean/blac051
Orbach, D. N., Hedrick, B., Würsig, B., Mesnick, S. L., & Brennan, P. L. R. (2018). The evolution of genital shape variation in female cetaceans. *Evolution*, *72*(2), 261–273. https://doi.org/10.1111/evo.13395
Orr, T. J., Lukitsch, T., Eiting, T. P., & Brennan, P. L. R. (2022). Testing Morphological Relationships Between Female and Male Copulatory Structures in Bats. *Integrative and comparative biology*, *62*(3), 602-612. https://doi.org/10.1093/icb/icac040
Plum, F. & Labonte, D. (2021). *scAnt*–an open-source platform for the creation of 3D models of arthropods (and other small objects) *PeerJ, 9.* e11155. https://doi.org/10.7717/peerj.11155
Rönn, J., Katvala, M., & Arnqvist, G. (2007). Coevolution between harmful male genitalia and female resistance in seed beetles. *Proceedings of the National Academy of Sciences of the United States of America*, *104*(26), 10921–10925. https://doi.org/10.1073/pnas.0701170104
Serna-Solis, V. (2022). Modularity and integration of copulatory structures in

male Ratfish, *Hydrolagus colliei* , Mount Holyoke Student Theses and Honors Collection. https://ida.mtholyoke.edu/handle/10166/6458

Stanley, H.P. (1963). Urogenital morphology in the chimaeroid fish Hydrolagus colliei (Lay and Bennett). *Journal of morphology, 112*(2), 99-127. https://doi.org/10.1002/jmor.1051120202